J. Micropalaeontology, 43, 283–302, 2024
https://doi.org/10.5194/jm-43-283-2024

Journal of Micropalaeontology
Open Access

Cambrian Furongian–Middle Ordovician conodonts in the northeastern margin of the South China Block (Chuzhou, Anhui province) and their paleogeographic implications

Bo Hu[1], Shuangying Li[1], Cheng Cheng[2], Min Li[1], Wei Xie[1], and Xing Wei[1]

[1]School of Resources and Environmental Engineering, Hefei University of Technology, Hefei 230009, China
[2]School of Geographic Science, Nantong University, Nantong 226019, China

Correspondence: Shuangying Li (lsysteven@126.com) and Cheng Cheng (15555138156@163.com)

Received: 16 January 2024 – Revised: 21 May 2024 – Accepted: 18 June 2024 – Published: 2 August 2024

Abstract. The South China Block is crucial for the global study of Cambrian to Ordovician conodont biostratigraphy, but research on its northeastern margin is relatively scarce. Chuzhou, located at the intersection of the South China Block, North China Block, and the Qinling–Dabie orogenic belt, boasts a significant thickness (> 1100 m) of carbonate-dominated sedimentary succession during the Cambrian Furongian to Middle Ordovician period. In this study, detailed field measurements and sample collection were conducted on two well-exposed sections in the Chuzhou area. Nine conodont biozones and three assemblages were identified from the Furongian Stage 10 to the Middle Ordovician Darriwilian, including the *Cordylodus proavus*, *Cordylodus lindstromi*, *Iapetoganathus fluctivagus*, *Cordylodus angulatus*, *Rossodus manitouensis*, *Colaptoconus quadraplicatus*, *Paltodus deltifer*, *Paroistodus proteus*, and *Triangulodus bifidus* zones, as well as the *Juanognathus anhuiensis–Protopanderodus gradates*, *Nasusgnathus giganteus–Paroistodus parallelus*, and *Dapsilodus virtualis–Protopanderodus robustus* assemblages. The analysis of conodont biogeographic zonation indicates that conodonts in the study area were predominantly from the North American Midcontinent Province (warm-water biota) and North Atlantic Province (cold-water biota) from Stage 10 to the middle Tremadocian and from the late Tremadocian to the Darriwilian, respectively. This conodont biogeographic transition is comparable to that in the Tarim, North China, and Qinling blocks but precedes that in the interior of the South China Block, likely associated with the Early–Middle Ordovician global paleogeographic and surface oceanic models that led to the changeover of ocean currents in the study area from warm to cold. Furthermore, the *Iapetognathus fluctivagus* zone, defined as the Ordovician lowest boundary, was first discovered in the Lower Yangtze region and revealed the distribution of this species in the South China Block. The discovery of *Parapanderodus lanceolatus* in the early Tremadocian suggests a possible exchange of seawater between the Yangtze and Tarim blocks.

1 Introduction

The Cambrian Furongian to Middle Ordovician is critical in the transition from the Cambrian evolutionary fauna to Paleozoic evolutionary fauna (Sepkoski, 1978, 1979, 1981, 1984; Harper et al., 2019). This epoch witnessed significant global changes in paleoclimate, paleoenvironment, paleogeography, and paleontology, including sea level fluctuations (Berner, 2001; Haq and Schutter, 2008), climate change (Trotter et al., 2008; Fang et al., 2019), carbon isotope anomalies (Schmitz et al., 2010; Zhu et al., 2006), and biodiversification events (Sepkoski and Sheehan, 1983; Sepkoski, 1995; Miller, 2003). Conodonts serve as crucial standard fossils from the Late Cambrian to the Ordovician, and the establishment of a conodont biostratigraphic framework facilitates precise temporal discussions of the aforementioned phenomena. The biogeographic zonation of conodonts is influenced by several factors, notably water depth (Seddon and Sweet, 1971; Sweet,

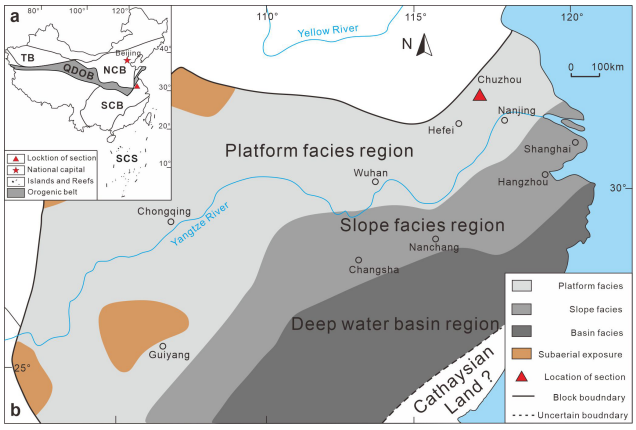

Figure 1. **(a)** Geotectonic framework map of the study area. TB is the Tarim Block, QDOB is the Qinling–Dabie orogenic belt, NCB is the North China Block, SCB is the South China Block, and SCS is the South China Sea, modified from Li et al. (2023). **(b)** Distribution map of sedimentary facies in the South China Block, modified from Munnecke et al. (2011).

1984; Zhen and Percival, 2003), temperature (Sweet and Bergström, 1972, 1984; Wang et al., 1996), salinity (Barnes and Fåhræus, 1975; Lindström, 1984), and tectonic movements (Pei, 2000), indicating significant paleogeographic implications (Zhan et al., 2013; Wu et al., 2014; Jing et al., 2015, 2017; Bergström and Ferritti, 2017; Wang et al., 2019).

Late Cambrian to Ordovician marine strata in the South China Block are extensively developed, well exposed, and fossil-rich. A large number of studies on conodonts has been done here since the 1980s (An, 1981, 1987; Ding, 1993; Dong, 1990, 1999; Dong et al., 2004; Wang, 1993; Wang et al., 1996), and the area still produces numerous studies for conodonts (Zhen et al., 2006; Wu et al., 2008, 2014; Wang and Wu, 2009; Wang et al., 2019; Gong et al., 2023). However, previous studies has primarily focused on the western and central parts of the South China Block (Upper Yangtze and Middle Yangtze regions), with relatively limited studies on the northeastern margin of the Lower Yangtze region. This limitation results in an incomplete conodont biostratigraphic framework in the South China Block, impeding regional stratigraphic correlations. Chuzhou, Anhui province, situated on the northeastern margin of the Lower Yangtze region, is the intersection of the South China Block, the North China Block, and the Qinling–Dabie orogenic belt (Fig. 1a). With its substantial thickness (> 1500 m) of Cambrian to Ordovician strata, well-exposed geological formations, and abundant paleontological species, Chuzhou represents an ideal area for investigating bioenvironmental events and paleogeographic evolution of the South China Block during this period. This study systematically conducted fieldwork and sample collection on the Cambrian Furongian–Middle Ordovician strata in the Chuzhou area to establish a conodont biostratigraphic sequence and discussed the influence of seawater depth, climate, water temperature, and ocean currents on the biogeographic zonation of conodonts, along with the paleogeographic implications of select conodont species.

2 Geological settings

During the Cambrian Furongian to the Middle Ordovician, the South China Block was situated in the middle to lower latitudes of the northern margin of the Gondwana landmass, adjacent to the Annamia, Sibumasu, and Tarim blocks (Torsvik and Cocks, 2013). Based on sedimentary facies distribution, the South China Block was subdivided, from northwest to southeast, into the Yangtze region (platform facies), the Jiangnan region (slope facies), and the Zhujiang region (basin facies) (Feng et al., 2001, 2003; Zhang et al., 2002; Wang, 2016; Wang and Zhan, 2023; Wang et al., 2023) (Fig. 1b). The Lower Yangtze region, situated in the northeastern part of the Yangtze region, lies between the southeastern margin of the Dabie Orogenic Belt and the Jiangnan Orogenic Belt. The Late Cambrian Furongian strata predominantly consist of shallow-water carbonate rocks, extending into early Early Ordovician and forming a carbonate platform characterized by thick dolomite and limestone deposits. However, the carbonate platform experienced significant reduction in the late Early Ordovician. By the Middle Ordovician, the carbonate platform became submerged due to rapidly rising sea levels, leading to increased terrigenous input and the formation of a mixed carbonate-clastic platform (Zhang et al., 2002; Feng et al., 2003).

The Chuzhou area is situated on the northeastern margin of the Lower Yangtze region. The Furongian–Middle Ordovician strata in this region are well exposed and extended in a NE–SW direction (Fig. 2). These formations primarily comprise carbonate rocks, with minor occurrences of mudstone and shale. The Daqishan quarry section (32°13′8.1″ N, 118°12′26.4″ E), approximately 13 km southwest of the Chuzhou urban area, exhibits a continuous stratigraphic succession from Cambrian Stage 10 to Ordovician Darriwilian with a huge thickness of 1113.9 m. On the other hand, the Langyashan section (32°16′24.0″ N, 118°17′43.4″ E) exposes Cambrian Furongian to Lower Ordovician strata with a thickness of 462.7 m. The lithostratigraphic units of these two sections are described in ascending order as follows.

2.1 Langyashan section

Langyashan Formation. The lower part of the Langyashan Formation is comprises gray medium- to thick-bedded limestone (Fig. 3a). The middle part of this formation is characterized by dark gray thick-bedded limestone with densely accumulated mud bands. The upper part consists of light gray thick-bedded dolomite. The Langyashan Formation has a total thickness of about 99.8 m and contains abundant trilobites, such as *Proceratiyge* and *Pseudopelaspis* (Zhu et al., 1984).

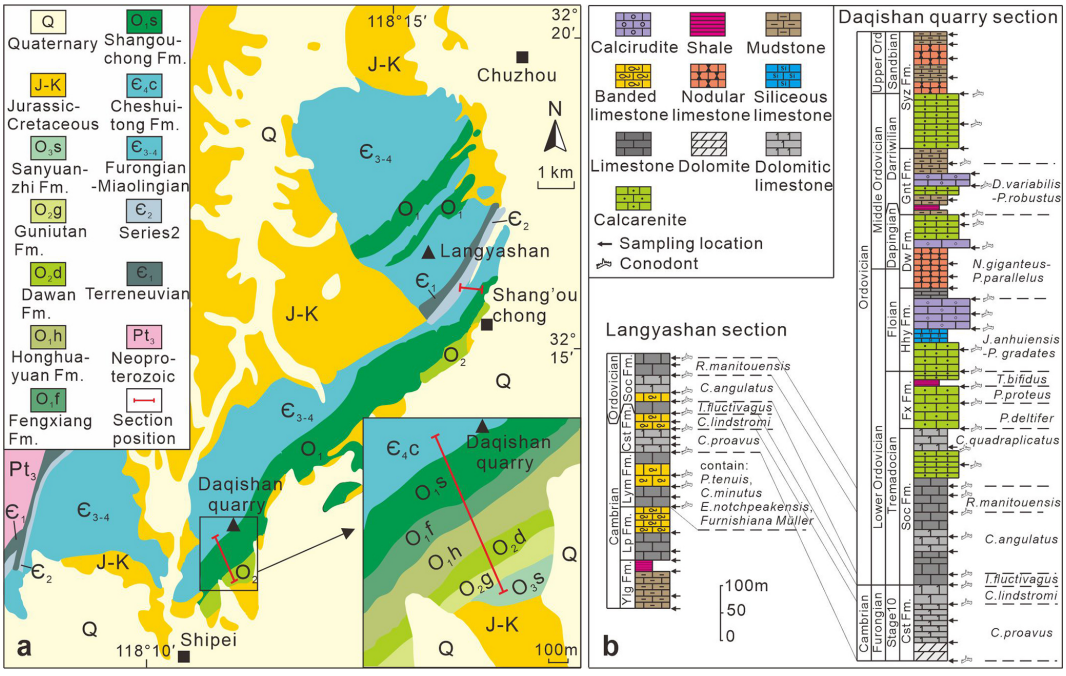

Figure 2. **(a)** Stratigraphic distribution map of Furongian to Middle Ordovician in Chuzhou area, modified from the Anhui Geological Bureau (1987). **(b)** Stratigraphic histogram of sections in the Chuzhou area. Cst is for Cheshuitong Fm (formation), Soc is for Shangouchong Fm, Fx is for Fenxiang Fm, Hhy is for Honghuayuan Fm, Dw is for Dawan Fm, Knt is for Kuniutan Fm, and Syz is for Sanyuanzhi Fm.

Cheshuitong Formation. The lower part of this Cheshuitong Formation primarily consists of dolomitic limestone with a total thickness of about 72.5 m (Fig. 3b). The upper part of this formation comprises dark gray thick-bedded limestone with well-developed lime mud bands. Each lime mud band is approximately 1 to 2 cm thick. In the upper part of the formation, trilobite species such as *Pagoda* major and *Saukid* were discovered (Anhui Provincial Geological Survey, 1987). Previously, the *Proconodontus* and *Cordylodus proavus* zones were established within the Cheshuitong Formation (Dong, 1987).

Shangouchong Formation. This formation is composed of dark gray thick-bedded limestone and gray dolomitic limestone (Fig. 3c). The layers exhibited are relatively flat and contain some siliceous nodules. The lower part of the formation is dominated by banded limestone, with each mud band approximately 0.2 to 1 cm thick and appearing grayish-yellow after weathering. A small number of brachiopods including *Apheortis meeki*, *Archaeorthis* sp., the cephalopods *Proteocameroceratidae*, and the crinoid stem *Hexagonocyclinus* were discovered in this area (Anhui Provincial Geological Survey, 1987). Previously, conodont zones and assemblages, including the *Cordylodus intermedius* and the *Cordylodus angulatus* zones and the *Scolopodus bassleri–Scolopodus tripletus* assemblage, were established within the Shangouchong Formation (Dong, 1987).

2.2 Daqishan section

Cheshuitong Formation. The lower part of the Cheshuitong Formation is characterized by gray–white thick-bedded silty dolomite. The middle part consists of gray medium-bedded dolomitic limestone. The layers generally exhibit stylolites and locally contain siliceous nodules. The upper part comprises light gray thick-bedded or massive dolomitic calcarenite limestone (Fig. 3b). Only minor bioclastic material was observed within this formation. With a total thickness of 133.2 m, the Cheshuitong Formation features a high content of lime mud, dolomite, rare fossils, and birdseye structures, suggesting a supratidal sabkha environment (Zhu et al., 1984).

Shangouchong Formation. The lower and middle parts of the Shangouchong Formation are characterized by gray thick-bedded to massive banded limestone. The upper part comprises gray thick-bedded bioclastic limestone with abundant trilobites and echinoderms. Its uppermost part consists of light gray thick-bedded silty dolomitic limestone (Fig. 3c), with a total thickness of 283.6 m. Featuring a high content of lime mud, strong dolomite lithification, rare fossils, and intense evaporation, the Shangouchong Formation is indicative of an intertidal or supratidal sabkha environment in an arid climate (Zhu et al., 1984; Zhan and Jin, 2007; Liu et al., 2011).

Fenxiang Formation. The Fenxiang Formation primarily comprises of gray medium- to thick-bedded calcarenite, with

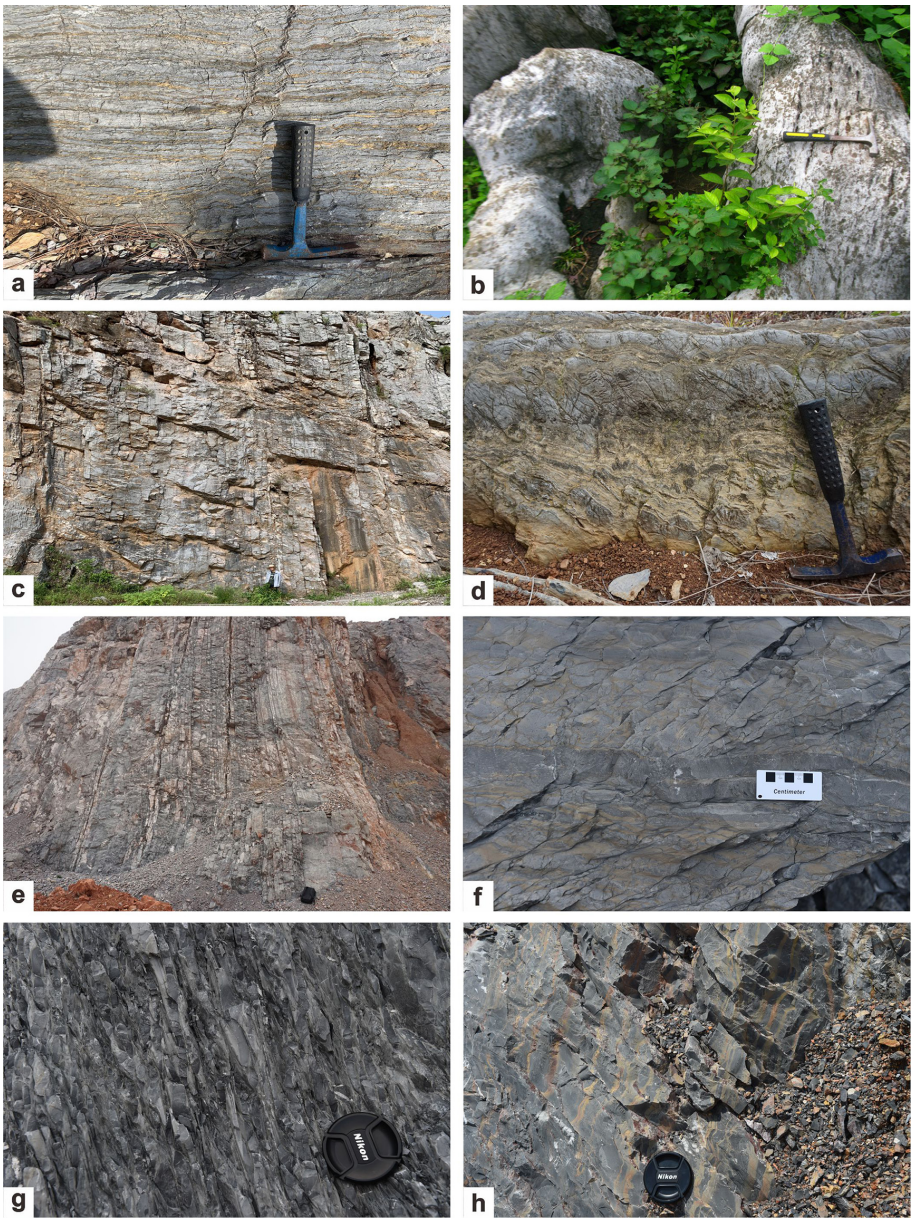

Figure 3. **(a)** Light gray medium to thick-bedded banded limestones of the middle part of the Langyashan Formation at Bed 6 of the Langyashan section. **(b)** Light gray massive dolomitic limestone of the upper part of the Cheshuitong Formation at Bed 3 of the Daqishan section. **(c)** Light gray thick-bedded to massive limestone or dolomitic limestone of the Shangouchong Formation at Bed 10 of the Daqishan section. **(d)** Thin gray to medium-bedded calcarenite interbedded with shales of the upper part of the Fenxiang Formation at Bed 12 of the Daqishan section. **(e)** Dark gray medium-bedded siliceous limestone of the middle part of the Honghuayuan Formation at Bed 15 of the Daqishan section. **(f)** Dark gray medium-bedded nodular limestone of the lower part of the Dawan Formation at Bed 18 of the Daqishan section. **(g)** Dark gray thin-bedded mudstone interbedded with shales in the middle part of the Kuniutan Formation at Bed 23 of the Daqishan section. **(h)** Dark thick-bedded calcarenites of the lower part of the Sanyuanzhi Formation at Bed 28 of the Daqishan section.

a total thickness of 103.0 m, often displaying a mottled reddish-brown weathered surface. The uppermost part of this formation mainly contains yellow–brown thin-bedded shale (Fig. 3d). The Fenxiang Formation is predominantly matrix-supported, with a higher content of bioclasts dominated by a few closed-species biological assemblages, suggesting a possible restricted platform or lagoon environment (Zhu et al., 1984; Liu et al., 2011).

Honghuayuan Formation. The lower part of the Honghuayuan Formation is characterized by dark gray thick-bedded bioclastic limestone containing fragments of echinoderms and trilobites. The middle part of this

formation comprises dark gray medium-bedded siliceous limestone, while the upper part contains gray thick-bedded calcarenite (Fig. 3e). With a total thickness of 144.4 m, the Honghuayuan Formation is mainly particle-supported grainstone. The grains are predominantly bioclastic, with a small number of intraclasts, indicating a highly hydrodynamic environment such as a mid-ramp or shoal (Liu, 2009; Liu et al., 2011).

Dawan Formation. The lower part of the Dawan Formation comprises dark gray medium-bedded nodular limestone, while the upper part consists of gray thick-bedded bioclastic calcarenite or calcirudite (Fig. 3f). With a total thickness of 138.7 m, the Dawan Formation features a higher content of lime mud and fewer bioclasts, with echinoderms dominating, suggesting relatively weak hydrodynamics and presumably a mid-ramp environment (Luan et al., 2019, 2021).

Kuniutan Formation. The base of the Kuniutan Formation comprises dark gray thin-bedded mudstone with interbedded shales. The lower part consists of dark gray thin-bedded silty limestone. The middle part comprises gray medium-bedded bioclastic calcarenite or calcirudite, while the upper part mainly comprises dark gray thin-bedded mudstone (Fig. 3g). With a total thickness of 112.1 m, the Kuniutan Formation is dominated by lime mudstone, with fine-grained bioclasts, suggestive of deposition in an outer-ramp environment (Zhan and Jin, 2007).

Sanyuanzhi Formation. The lower part of the Sanyuanzhi Formation is composed of dark gray thick-bedded calcarenites. The upper part is interbedded with dark gray medium- to thick-bedded nodular limestones and mudstones (Fig. 3h). No fossil records are associated with this formation. The Sanyuanzhi Formation consists entirely of lime mudstone with minor particles, suggesting a formation on an outer ramp where the waterbody is deeper (Zhu et al., 1984; Luan et al., 2018).

3 Materials and methods

A total of 60 limestone or dolomite conodont samples, each weighing approximately 2 to 5 kg, were collected in the Daqishan quarry section (39) and the Langyashan section (21). There are 36 samples yielding conodonts. The richest specimens came from the lower part of the succession (Cheshuitong, Shangouchong, and Fenxiang formations); however, few were yielded in the upper part (Dawan and Kuniutan formations). Conodont separation was performed at the Micropaleontology Laboratory, School of Resource and Environmental Engineering, Hefei University of Technology, China. All samples were cleaned, crushed to 1–2 cm^3, and then dissolved with 5 %–10 % diluted acetic acid to obtain insoluble residues (Jeppsson et al., 1999). Residues were collected by wet sieving through 60 and 160 meshes and air-dried, after which conodonts were handpicked using a binocular microscope. All specimens were deposited at the Micropaleontology Lab of the Hefei University of Technology, and selected forms were photographed using scanning electron microscopy (SEM).

4 Results

4.1 Conodont fauna and biostratigraphy

A total of 473 conodont elements were recovered and assigned to 45 species and 28 genera from the Cambrian Stage 10 to the Ordovician Darriwilian (Figs. 4, 5). The sample number, position, species, and amount are provided in the Supplement.

4.1.1 Langyashan section

The conodont biostratigraphy from the Cambrian Stage 10 to the Ordovician Tremadocian established from the Langyashan section is as follows (Fig. 6).

Cordylodus proavus zone:

The *C. proavus* zone was first established in the North American carbonate platform facies in the House Range, Utah (Miller, 1969, 1980). This biozone is located in the middle and lower part of the Cheshuitong Formation (Bed 8) with the occurrence of *Cordylodus proavus* as the bottom boundary and *Cordylodus lindstromi* as the top boundary. Other symbiotic species include *Cambrooistodus cambricus*, *Phakelodus tenuis*, *Proconodontus muelleri*, *Furnishina furnishi*, *Proconodontus tenuiserratus*, *Eoconondontus notchpeakensis*, *Cordylodus intermedius*, and *Monocostodus sevierensis* (Fig. 4).

Cordylodus lindstromi zone:

The *C. lindstromi* zone was first established in the North American biozone (Miller, 1980). This biozone is located at the top of the Cheshuitong Formation (Bed 9) with the occurrence of *Cordylodus lindstromi* as its bottom boundary and the occurrence of *Iapetognathus fluctivagus* as its top boundary. The conodonts in this zone are *Chosonodina tridentata*, *Teridontus nakamurai*, *Teridontus gracilis*, *Teridontus erectus, Utahconus beimadaoensis*, and *Drepanodus tenuis* (Fig. 4).

Iapetognathus fluctivagus zone:

The *I. fluctivagus* zone was first established in Green Point, Newfoundland (Barnes, 1988; Cooper et al., 2001). This biozone is located at the bottom of the Shangouchong Formation (Bed 10) with the occurrence of *Iapetognathus fluctivagus* as the bottom boundary and the occurrence of *Cordylodus angulatus* as the top boundary. Conodonts in this zone also include *Moncostodus sevierensis*, *Teridontus nakamurai*, *Teridontus gracilis*, *Cordylodus intermedius*, *Acanthodus lineatus*, *Teridontus erectus*, and *Drepanodus tenuis* (Fig. 4).

Cordylodus angulatus zone:

The *C. angulatus* zone was first established in the North American biozone (Miller, 1978). This biozone is located in

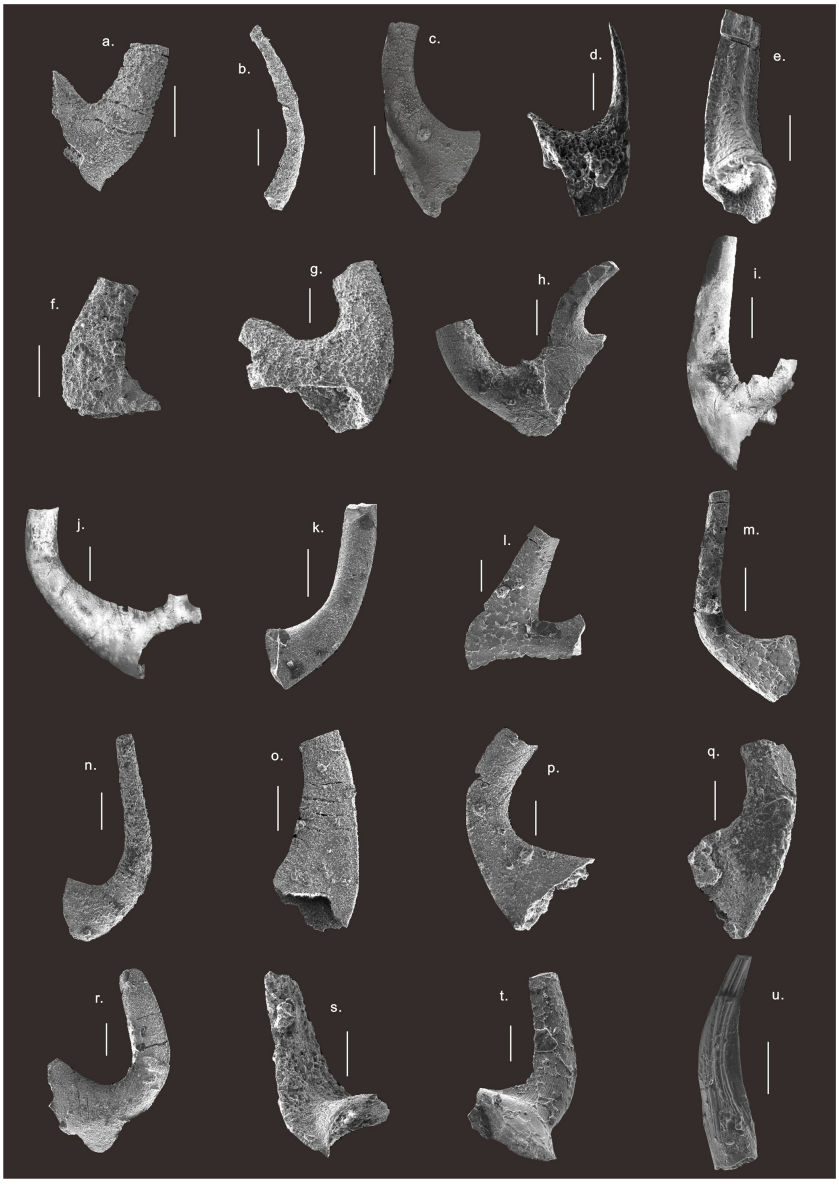

Figure 4. SEM photos of conodonts from the Chuzhou area. **(a)** *Cambrooistodus cambricus* (Miller, 1969) from sample wz882 of the Langyashan Formation. **(b)** *Phakelodus tenuis* (Müller, 1959) from sample wz885 of the Langyashan Formation. **(c)** *Proconodontus muelleri* (Miller, 1969) from sample wz886 of the Langyashan Formation. **(d)** *Furnishina furnishi* (Müller, 1959) from sample wz887 of the Langyashan Formation. **(e)** *Utahconus utahensis* (Miller, 1969) from sample wz890 of the Cheshuitong Formation. **(f)** *Utahconus beimadaoensis* (Chen, 1988), S element, from sample wz892 of the Cheshuitong Formation. **(g)** *Cordylodus angulatus* (Pander, 1856), Pb element, from sample wz910 of the Shangouchong Formation. **(h)** *Cordylodus intermedius* (Furnish, 1938), S element, from sample wz897 of the Cheshuitong Formation. **(i)** *Cordylodus lindstromi* (Druce and Jones, 1971), S element, from sample wz897 of the Cheshuitong Formation. **(j)** *Cordylodus proavus* (Müller, 1959), S element, from sample wz892 of the Cheshuitong Formation. **(k)** *Monocostodus sevierensis* (Miller, 1969) from sample wz904 of the Shangouchong Formation. **(l)** *Iapetognathus fluctivagus* (Nicoll et al., 1999), P element, from sample wz904 of the Shangouchong Formation. **(m)** *Teridontus huanghuachangensis* (Ni, 1981), S element, from sample wz904 of the Shangouchong Formation. **(n)** *Teridontus nakamurai* (Nogami, 1967), S element, from sample wz916 of the Shangouchong Formation. **(o)** *Teridontus erectus* (Druce and Jones, 1971), S element, from the sample wz907 of the Shangouchong Formation. **(p)** *Drepanodus tenuis* (Moskalenko, 1967), P element, from sample wz910 of the Shangouchong Formation. **(q)** *Drepanoistodus suberectus* (Branson and Mehl, 1933), Sa element, from sample wz910 of the Shangouchong Formation. **(r)** *Scolopodus primitivus* (An et al., 1983), S element, from sample wz925 of the Shangouchong Formation. **(s)** *Semiacontiodus baianensis* (Ding, 1993), S element, from sample wz917 of the Shangouchong Formation. **(t)** *Semiacontiodus lavadamensis* (Miller, 1969) from sample wz945 of the Shangouchong Formation. **(u)** *Parapanderodus lanceolatus* (Ji and Barnes, 1994), Sa element, from sample wz923 of the Shangouchong Formation.

Figure 5. SEM photos of conodonts from the Chuzhou area. **(a)** *Parapanderodus striatus* (Graves and Ellison, 1941), Sa element, from sample wz924 of the Shangouchong Formation. **(b)** *Rossodus manitouensis* (Repetski and Ethington, 1983), S element, from sample wz929 of the Shangouchong Formation. **(c)** *Variabiloconus bassleri* (Furnish, 1938), S element, from sample wz923 of the Fenxiang Formation. **(d)** *Colaptoconus quadraplicatus* (Branson and Mehl, 1933), S element, from sample wz923 of the Shangouchong Formation. **(e)** *Acodus jiangningensis* (Ding, 1993) from sample wz917 of the Shangouchong Formation. **(f)** *Paltodus deltifer* (Lindström, 1955) from sample wz935 of the Fenxiang Formation. **(g)** *Triangulodus proteus* (An, 1981), S element, from sample wz961 of the Honghuayuan Formation. **(h)** *Cornuodus longibasis* (Lindström, 1955), Sa element, from sample wz976 of the Dawan Formation. **(i)** *Paroistodus parallelus* (Pander, 1856), Sc element, from sample wz978 of the Dawan Formation. **(j)** *Juanognathus anhuiensis* (An, 1987), S element, from sample wz961 of the Honghuayuan Formation. **(k)** *Scolopodus fangcunensis* (Ding, 1993), S element, from sample wz972 of the Honghuayuan Formation. **(l)** *Triangulodus brevibasis* (Sergeeva, 1963), Sb element, from sample wz950 of the Honghuayuan Formation. **(m)** *Dapsilodus variabilis* (Webers, 1966), S element, from sample wz995 of the Kuniutan Formation. **(n)** *Scalpellodus tersus* (Dzik, 1976), S element, from sample wz935 of the Fenxiang Formation. **(o)** *Protopanderodus gradatus* (Serpagli, 1974), S element, from sample wz954 of the Honghuayuan Formation. **(p)** *Nasusgnathus giganteus* (Ni and Li, 1987), Sb element, from sample wz978 of the Dawan Formation. **(q)** *Protopanderodus robustus* (Hadding, 1913), Sa element, from sample wz1002 of the Kuniutan Formation. **(r)** *Protopanderodus varicostatus* (Sweet and Bergström, 1962), S element, from sample wz1002 of the Kuniutan Formation. **(s)** *Drepanodus arcuatus* (Pander, 1856), Sa element, from sample wz983 of Dawan Formation. **(t)** *Drepanoistodus basiovalis* (Sergeeva, 1963), Sa element, from sample wz999 of Kuniutan Formation. **(u)** *Scabbardella altipes* (Henningsmoen, 1948), P element, from sample wz1005 of Sanyuanzhi Formation. Scale bars = 100 µm. All specimens are preserved in the Micropaleontology Lab at the Hefei University of Technology.

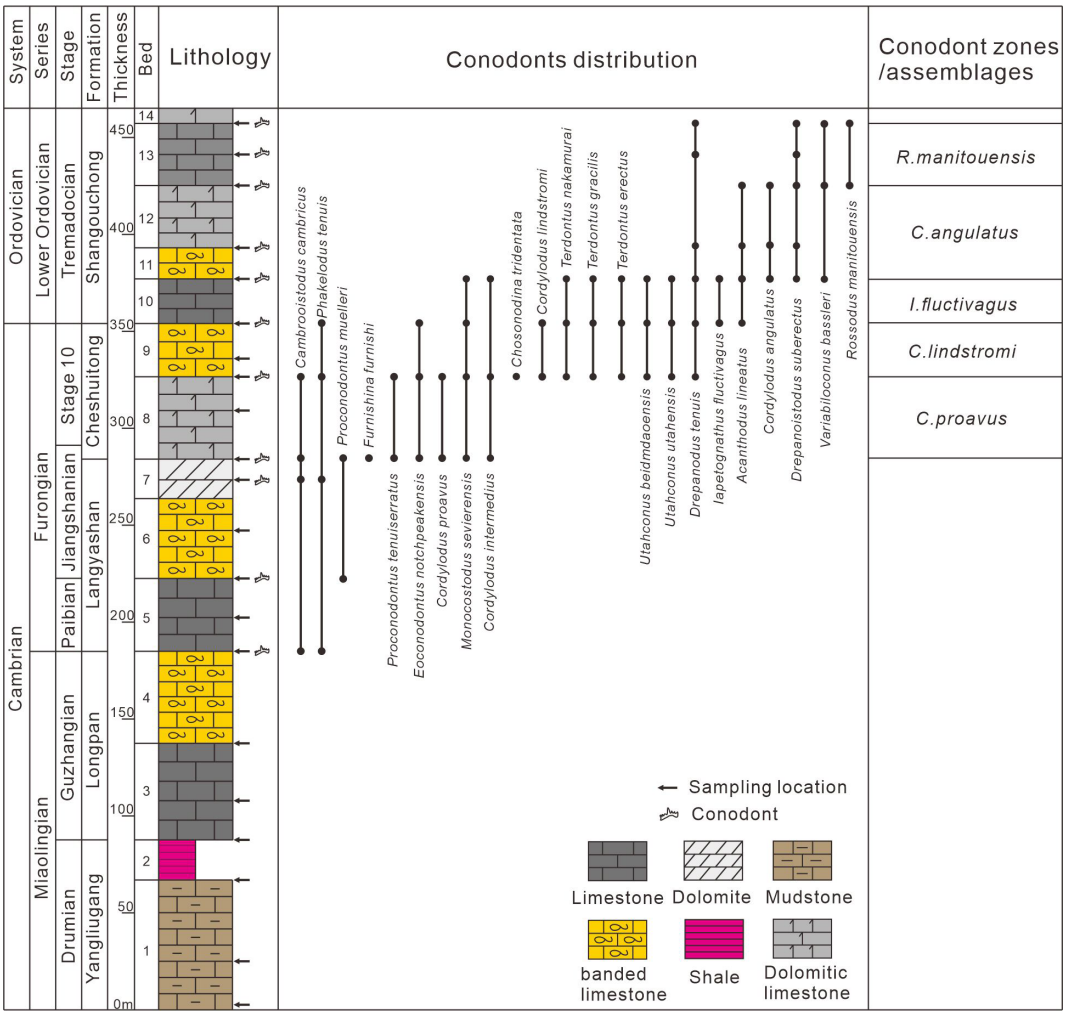

Figure 6. Cambrian Furongian–Lower Ordovician conodont biostratigraphy in the Langyashan Section.

the lower part of the Shangouchong Formation (Bed 11 to 12) with the occurrence of *Cordylodus angulatus* as the bottom boundary and the occurrence of *Rossodus manitouensis* as the top boundary. Conodonts in this zone also include *Scolopodus pseudoplanus*, *Semiacontiodus baianensis*, *Acanthodus lineatus*, *Drepanodus tenuis*, *Drepanoistodus suberectus*, and *Variabiloconus bassleri* (Figs. 4, 5).

Rossodus manitouensis zone:

The *R. manitouensis* zone was first established in the North American biozone (Pyle and Barnes, 2001). This biozone is located in the middle of the Shangouchong Formation (Bed 13) with the occurrence of *Rossodus manitouensis* as the bottom boundary and the occurrence of *Colaptoconus quadraplicatus* as the top boundary. Conodonts in this zone also include *Scolopodus primitivus*, *Variabiloconus bassleri*, *Aloxoconus staufferi*, *Acanthodus lineatus*, *Drepanodus tenuis*, *Drepanoistodus suberectus*, *Scolopodus pseudoplanus*, and *Parapanderodus striatus* (Figs. 4 and 5).

4.1.2 Daqishan quarry section

The conodont biostratigraphy from the Cambrian Stage 10 to the Ordovician Darriwilian in the Daqishan quarry section is as follows (Fig. 7).

Cordylodus proavus zone:

This biozone is located in the middle and lower part of the Cheshuitong Formation (Bed 1 to 2) with the occurrence of *Cordylodus proavus* as the bottom boundary and *Cordylodus lindstromi* as the top boundary. Conodonts in this zone also include *Phakelodus tenuis*, *Utahconus beimadaoensis*, *Cordylodus intermedius*, *Teridontus nakamurai*, *Teridontus gracilis*, and *Monocostodus sevierensis* (Fig. 4).

Cordylodus lindstromi zone:

This biozone is located at the top of the Cheshuitong Formation (Bed 3) with the occurrence of *Cordylodus lindstromi* as the bottom boundary and the occurrence of *Iapetognathus fluctivagus* as the top boundary. Conodonts in this zone also include *Moncostodus sevierensis*, *Teridontus erectus*, *Teri-*

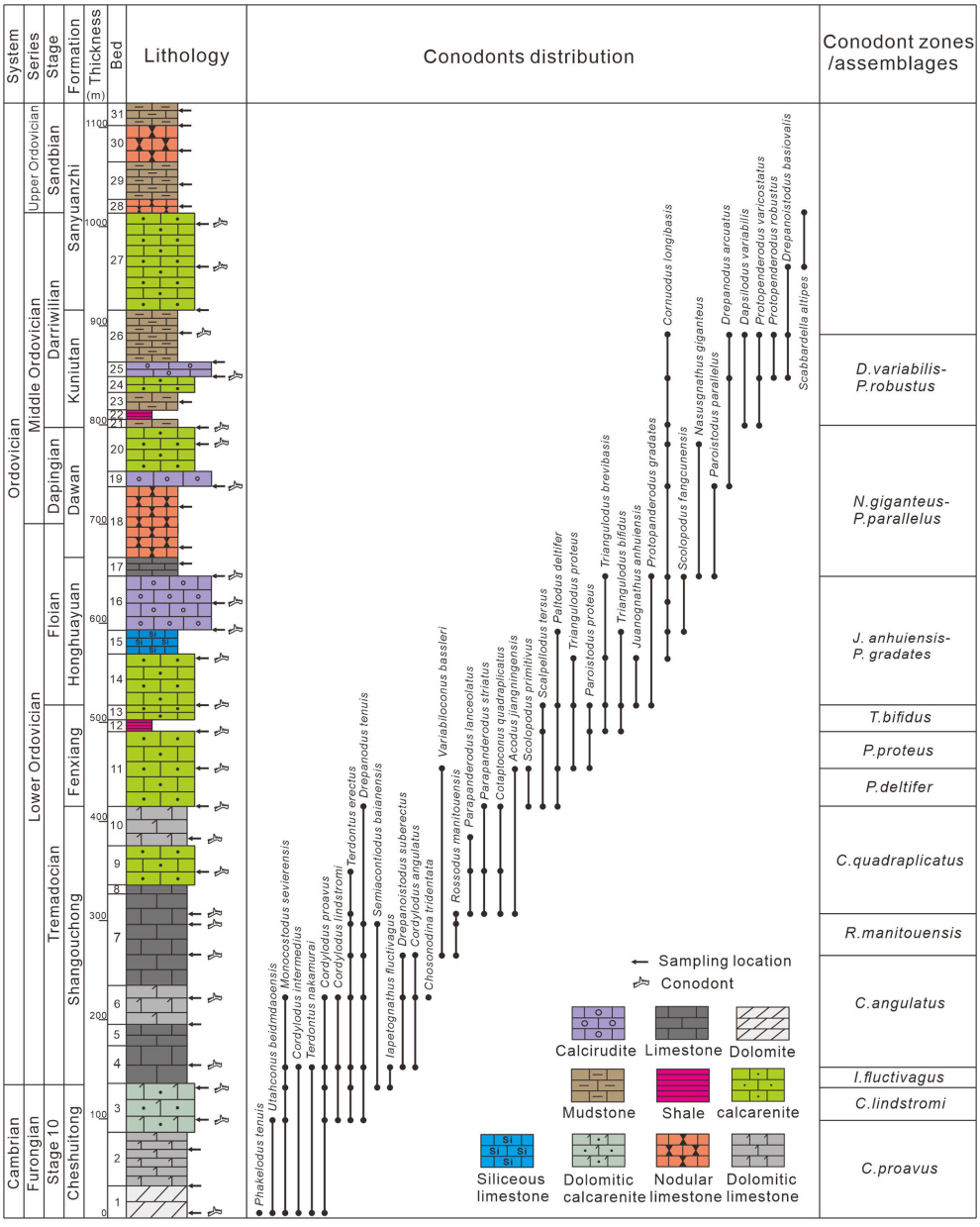

Figure 7. Cambrian Furongian–Middle Ordovician conodont biostratigraphy in the Daqishan quarry section.

dontus nakamurai, *Teridontus gracilis*, *Cordylodus proavus*, and *Cordylodus intermedius* (Fig. 4).

Iapetognathus fluctivagus zone:

This biozone is located at the bottom of the Shangouchong Formation (the lower part of Bed 4) with the occurrence of *Iapetognathus fluctivagus* as the bottom boundary and the occurrence of *Cordylodus angulatus* as the top boundary. Conodonts in this zone also include *Moncostodus sevierensis*, *Teridontus nakamurai*, *Teridontus gracilis*, *Teridontus erectus*, *Cordylodus proavus*, *Cordylodus intermedius*, *Acanthodus lineatus*, *Semiacontiodus baianensis*, *Cordylodus lindstromi*, and *Drepanodus tenuis* (Fig. 4).

Cordylodus angulatus zone:

This biozone is located at the lower part of the Shangouchong Formation (upper part of Bed 4 to lower part of Bed 7) with the occurrence of *Cordylodus angulatus* as the bottom boundary and the occurrence of *Rossodus manitouensis* as the top boundary. Conodonts in this zone also include *Scolopodus pseudoplanus*, *Chosonodina tridentata*, *Teridontus gracilis*, *Teridontus erectus*, *Aloxoconus staufferi*, *Acanthodus lineatus*, *Drepanodus tenuis*, *Drepanoistodus suberectus*, and *Variabiloconus bassleri* (Fig. 4).

Rossodus manitouensis zone:

This biozone is located in the middle of the Shangouchong Formation (the upper part of Bed 7) with the occurrence of *Rossodus manitouensis* as the bottom boundary and the occurrence of *Colaptoconus quadraplicatus* as the top boundary. Conodonts in this zone also include *Variabiloconus bassleri*, *Aloxoconus staufferi*, *Teridontus erectus*, *Drepanodus tenuis*, *Drepanoistodus suberectus*, and *Scolopodus pseudoplanus* (Figs. 4, 5).

Colaptoconus quadraplicatus zone:

The *C. quadraplicatus* zone was first established in the North American biozone (Branson and Mehl, 1933). This biozone is located at the top of the Shangouchong Formation (Bed 8 to Bed 10) with the occurrence of *Colaptoconus quadraplicatus* as the bottom boundary and *Paltodus deltifer* as the top boundary. Conodonts in this zone also include *Acodus jiangningensis*, *Teridontus erectus*, *Drepanodus tenuis*, *Scolopodus primitivus*, *Rossodus manitouensis*, *Variabiloconus bassleri*, *Parapanderodus striatus*, and *Parapanderodus lanceolatus* (Fig. 5).

Paltodus deltifer zone:

The *P. deltifer* zone was first established in the Baltic (Lindström, 1971). This biozone is located at the bottom of the Fenxiang Formation (lower part of Bed 11) with *Paltodus deltifer* as the bottom boundary and *Paroistodus proteus* as the top boundary. Conodonts in this zone also include *Acodus jiangningensis*, *Drepanodus tenuis*, *Scolopodus primitivus*, *Variabiloconus bassleri*, and *Scalpellodus tarsus* (Fig. 5).

Paroistodus proteus zone:

The *P. proteus* zone was first established in Europe (Lindström, 1971). This biozone is located in the middle of the Fenxiang Formation (upper part of Bed 11) with the occurrence of *Paroistodus proteus* as the bottom boundary and the occurrence of *Triangulus bifidus* as the top boundary. Conodonts in this zone also include *Paltodus sweeti*, *Scalpellodus tarsus*, *Scolopodus pseudoplanus*, *Triangulodus proteus*, and *Paltodus deltifer* (Fig. 5).

Triangulodus bifidus zone:

The *T. bifidus* zone was first established in South China (Zhen et al., 2006). This biozone is located at the top of the Fenxiang Formation (Bed 12 to Bed 13) with the occurrence of *Triangulus bifidus* as the bottom boundary. Conodonts in this zone also include *Scolopodus pseudoplanus*, *Scalpellodus tarsus*, *Paltodus deltifer*, *Paroistodus proteus*, *Triangulodus proteus*, *Paltodus sweeti*, and *Triangulodus brevibasis* (Fig. 5).

Juanognathus anhuiensis–Protopanderodus gradates assemblage:

The assemblage is located in the Honghuayuan Formation (Bed 14 to Bed 16) which is defined by the co-occurrence of *Juanognathus anhuiensis–Protopanderodus gradates*. Conodonts in this assemblage also include *Scolopodus fangcunensis*, *Paltodus deltifer*, *Triangulodus bifidus*, *Triangulodus brevibasis*, *Scolopodus rex*, and *Cornuodus longibasis* (Fig. 5).

Nasusgnathus giganteus–Paroistodus parallelus assemblage:

This assemblage is located in the Dawan Formation (Bed 17 to Bed 20) which is defined by the co-occurrence of *Nasusgnathus giganteus–Paroistodus parallelus*. Conodonts in this assemblage also include *Drepanodus arcuatus*, *Triangulodus brevibasis*, *Scolopodus rex*, and *Cornuodus longibasis* (Fig. 5).

Dapsilodus viruensis–Protopanderodus robustus assemblage:

This assemblage is located in the Kuniutan Formation (Bed 21 to Bed 26) which is defined by the co-occurrence of *Dapsilodus viruensis–Protopanderodus robustus*. Conodonts in this assemblage also include *Drepanodus arcuatus*, *Paroistodus parallelus*, *Protopanderodus varicostatus*, *Cornuodus longibasis*, and *Protopanderodus variabilis* (Fig. 5).

5 Discussion

5.1 Regional correlation of conodont zones

The conodont zones established from the Cambrian Furongian to Middle Ordovician Darriwilian in the Chuzhou area can be well correlated with the conodont zones from the adjacent blocks. The detailed descriptions are as follows.

Cordylodus proavus zone:

The zone fossil *C. proavus* is a globally distributed species, which is widely distributed in Cambrian Furongian strata in the South China Block and North China Block (Wang et al., 2016, 2019), and can be correlated with the lower part of the *T. Nakamurai–T. huanghuachangensis–T. gracilis* assemblage in the Tarim Block (Table 1). The main members of this conodont zone are *P. tenuis*, *U. beimadaoensis*, *U. utahensis*, *C. intermedius*, *T. nakamurai*, *T. gracilis*, and *M. sevierensis*.

Cordylodus lindstromi zone:

The zone fossil *C. lindstromi* is common in the Cambrian Furongian strata of the North China Block and also distributed in the Jiangnan region of the South China Block (Wang et al., 2014, 2016, 2019). This conodont zone corresponds to the lower part of the *M. sevierensis* zone of the Yangtze platform in the South China Block, which is equivalent to the lower part of the *T. Nakamurai–T. huanghuachangensis–T. gracilis* assemblage in the Tarim Block (Table 1). The main members of this conodont zone are *U. beimadaoensis*, *M. sevierensis*, *T. nakamurai*, *T. gracilis*, *C. proavus*, *C. intermedius*, *A. lineatus*, and *S. baianensis*.

Iapetognathus fluctivagus zone:

The zone fossil *I. fluctivagus* is globally restricted and defines the lowest boundary of the Ordovician (Barnes, 1988; Cooper et al., 2001). It has been noticed only in certain sections with low abundances (Nicoll et al., 1999; Miller et al., 2014, 2015; Albanesi et al., 2015; Zhen et al., 2017; Zhang et al., 2019). In the South China Block, the *I. fluctivagus* zone

Table 1. Correlation of Furongian Stage 10 to Middle Ordovician Darriwilian conodont biostratigraphy in the Daqishan quarry section with those from Langyashan (Dong, 1987), South China (Wang et al., 2019), North China (Wang et al., 2014), Tarim (Jing, 2009), and Qinling (Pei, 2000).

Series	Stage	Formation	Daqishan quarry, Chuzhou (this study)	Langyashan, Chuzhou	South China		Qinling	Tarim	North China
					Jiangnan slope	Yangtze platform			
Upper Ord.	Sandbian	Sanyuanzhi			*P. anserinus*	*Y. jianyeensis–P. anserinus*	*P. anserinus*	*P. anserinus*	*P. anserinus*
Middle Ordovician	Darriwilian	Kunitan	*D. variabilis–P. robustus* (assemblage)		*P. serra*	*P. serra*	*P. serra*	*P. serra*	*P. serra*
									P. anitae
					H. kristnae	*E. suecicus*	*E. suecicus*	*E. suecicus*	*E. suecicus*
					H. holodentata	*E. pseudoplanus–D. tablepointensis*		*Y. crassus*	*H. holodentata–T. tangshanensis*
					Y. crassus	*Y. crassus*			
					P. orginalis	*L. variabilis*	*L. variabilis*	*L. variabilis*	
						L. antivariabilis		*M. parva*	
	Dapingian	Dawan	*N. giganteus–P. parallelus* (assemblage)			*M. parva*	*P. orginalis*	*A. iaptosomatus–L. dissectus*	
						P. orginalis			
					?	*B. navis*		*S. chuxianensis–S. euspinus*	
						B. triangularis			
Lower Ordovician	Floian	Honghuayuan	*J. anhuiensis–P. gradates* (assemblage)		*O. evae*	*O. communis/O. evae*	*O. evae*	*S. diversus–S. tarimensis–P. proteus*	*J. gananda*
									P. obesus
					P. elegans				
						P. honghuayuanensis			*S. extensus*
				S. diversus	*S. bilobatus*	*S. diversus*	*P. elegans*		*S. bilobatus*
	Tremadocian	Fenxiang	*T. bifidus*	*S. bilobatus*	*T. bifidus*	*T. bifidus*	*P. proteus*	*T. proteus–P. deltifer*	*S. tersus–T.bifidus*
			P. proteus		*P. proteus*	*T. proteus–C. quadraplicatus*			
			P. deltifer	*P. deltifer*	*P. deltifer*		*P. deltifer*		
		Shangouchong	*C. quadraplicatus*	*S. bassleri–S. triplicatus*				*G. floweri*	*C. quadraplicatus*
								C. quadraplicatus	
			R. manitouensis	*C. angulatus*	*C. herfurthi*	*R. manitouensis*		*C. herfurthi–R. manitouensis*	*C. herfurthi–R. manitouensis*
			C. angulatus		*C. angulatus*	*C. angulatus*	*C. angulatus*		*C. angulatus*
				C. intermedius				*T. nakamurai–T. huanghuachangensis–T.gracilis*	*I. jilinensis*
			I. fluctivagus		*I. fluctivagus*	*M. sevierensis*			
Furongian	Stage 10	Cheshuitong	*C. lindstromi*	*C. proavus*	*C. lindstromi*				*C. lindstromi*
			C. proavus		*C. intermedius*	*C. proavus*			*C. proavus*
				Proconodontus	*C. proavus*				

is only found in Jiangnan region, which has a specific significance as an environmental indicator and corresponds to the *I. jilinensis* zone in the North China Block (Table 1). In this conodont zone, elements predominantly found in the Upper Cambrian to the Lower Ordovician include *M. sevierensis*, *T. nakamurai*, *T. gracilis*, *C. proavus*, *C. intermedius*, *A. lineatus*, *C. lindstromi*, *D. tenuis*, and *D. suberectus*.

Cordylodus angulatus zone:

The zone fossil *C. angulatus* is distributed worldwide in the lower part of the Lower Ordovician (Pei, 2000; Wang et al., 2016, 2019). The conodont zone established in this area is well correlated with that from the South China Block, North China Block, Tarim Block, and Qinling Block (Table 1). The main members of this conodont zone include *S. pseudoplanus*, *C. tridentata*, *T. gracilis*, *T. erectus*, *C. intermedius*, *D. tenuis*, *D. suberectus*, and *V. bassleri*.

Rossodus manitouensis zone:

The zone fossil *R. manitouensis* is mainly distributed in the Lower Ordovician of the South China Block (Lunshan Formation, Liuxia Formation, and Nanjinguan Formation), the North China Block (Yeli Formation), and the Tarim Block (Qulitage Group) (Wang et al., 2016, 2019). The *R. manitouensis* zone established in this area is equivalent to the *C. herfurthi* zone of the Jiangnan slope and the upper part of the *C. herfurthi–R. manitouensis* zone in the Tarim Block (Jing, 2009; Wang et al., 2019), which corresponds to the same name zone from the Yangtze platform (Table 1). The main members of this conodont zone include *S. primitivus*, *V. bassleri*, *A. staufferi*, *D. suberectus*, *T. erectus*, *S. pseudoplanus*, *C. angulatus*, and *P. striatus*.

Colaptoconus quadraplicatus zone:

The zone fossil *C. quadraplicatus* is distributed in the Lower Ordovician of the South China Block (Lunshan Formation), North China Block (Yeli Formation), and Tarim Block (Qulitage Group) (Jing, 2009; Wang et al., 2016, 2019). The *C. quadraplicatus* zone established in this area correlates with the lower part of the *T. proteus–C. quadraplicatus* zone from the Yangtze platform of the South China Block. It also corresponds to the same name zone of the North China Block and the Tarim Block (Table 1). The main members in the conodont zones are *S. rectus*, *A. jiangningensis*, *Teridontus erectus*, *D. tenuis*, *T. erectus*, *S. pseudoplanus*, and *R. manitouensis*.

Paltodus deltifer zone:

P. deltifer is a zone fossil that is widely distributed in many regions around the world (Pei, 2000; Wang et al., 2019). The *P. deltifer* zone established in this area corresponds to the upper part of the same name zone in the Qinling Block, Jiangnan Slope region, and the lower part of the *T.proteus–P. deltifer* zone in the Tarim Block. This conodont zone has not been found in the North China Block but can contrast with the lower part of the *S. tersus–T. bifidus* zone (Table 1). The key members of this conodont zone include *T. proteus*, *J. anhuiensis*, *T. erectus*, *D. tenuis*, *S. primitivus*, *T. brevibasis*, and *S.tersus*.

Paroistodus proteus zone:

The zone fossil *P. proteus* is mainly distributed in the South China Block and the Tarim Block, and it has also been found in the Qinling Block (Pei, 2000; Jing, 2009; Wang et al., 2019). The *P. proteus* zone established in this study corresponds to the same name zone on the Jiangnan Slope region and the upper part of the *T. proteus–C. quadraplicatus* zone in the Yangtze platform region. In addition, this zone corresponds to the middle part of the *S. tarsus–T. bifidus* zone in the North China Block, the middle part of the *T. proteus–P. deltifer* zone in the Tarim Block, and the lower part of the same name zone in the Qinling Block (Table 1). This conodont zone mainly contains *P. sweeti*, *P. gradates*, *C. longibasis*, *S. pseudoplanus*, *S. rex*, *A. jiangningensis*, *T. proteus*, *J. anhuiensis*, and *P. deltifer*.

Triangulodus bifidus zone:

The zone fossil *Triangulodus bifidus* is mainly distributed in the Lower Ordovician Fenxiang Formation and Honghuayuan Formation of the South China Block and the Lower Ordovician Qulitage group of the Tarim Block (Zhao and Tan, 1999; Wang et al., 2019). The *T. bifidus* zone established in this area corresponds to the same name zone in the South China Block, the upper part of the *S.tersus–T.bifidus* zone in the North China Block, the upper part of the *T.proteus–P.deltifer* zone in the Tarim Block, and the upper part of the same name zone in Qinling Block (Table 1). This conodont zone mainly contains *S. pseudoplanus*, *J. anhuiensis*, *P. deltifer*, *P. proteus*, *T. proteus*, *P. sweeti*, *P. gradates*, *S. rex*, and *C. longibasis*.

Juanognathus anhuiensis–Protopanderodus gradates assemblage:

Juanognathus anhuiensis and *Protopanderodus gradates* was mainly found in the Honghuayuan Formation and Dawan Formation (Lower to Middle Ordovician) of the Lower Yangtze region (Wang and Wu, 2009). The *J. anhuiensis–Protopanderodus gradates* assemblage established in this area corresponds to the *S. bilobatus* to *P. elegans* zone in the Jiangnan Slope region and the *S. diversus* to *O. communis* zone in the Yangtze platform region. It is comparable to the *S. bilobatus* to *P. obesus* zone in the North China Block and the *S. diversus–S. tarimensis–P. proteus* zone in the Tarim Block. It also correlates the *P. elegaus* zone to the lower–middle part of the *O. evae* zone in the Qinling Block (Table 1). The critical members of this conodont zone are *V. bassleri*, *P. deltifer*, *T. bifidus*, *T. brevibasis*, *C. longibasis*, and *P. parallelus*.

Nasusgnathus giganteus–Paroistodus parallelus assemblage:

N. giganteus was produced in the Lower and Middle Ordovician of the Yangtze platform region and Tarim Block. Similarly, *P. parallelus* was observed in the Dawan Formation (Middle Ordovician) from South China and the Qiulitag Group in the Tarim Block (Wang and Wu, 2009). The *N. giganteus–P. parallelus* assemblage established in the study area corresponds to the upper part of the *O. evae* zone and

the lower part of the *P. originalis* zone in the Jiangnan Slope region, the *O. evae* to the *M. parva* zone in the Yangtze platform region, the upper part of the *S. diversus–S. tarimensis–P. proteus* assemblage in the Tarim Block, and the upper part of the *O. evae* to *P. originalis* zone in the Qinling Block (Table 1). This conodont zone mainly contains *S. rex*, *C. longibasis*, and *J. jaanussoni*.

Dapsilodus viruensis–Protopanderodus robustus assemblage:

D. viruensis was mainly produced in the Kuniutan Formation (Middle Ordovician) and Yanwashan Formation (Upper Ordovician) in the South China Block, while *P. robustus* was primarily found in the Middle and Upper Ordovician in the South China Block, North China Block, and Tarim Block (Wang and Wu, 2009). The *D. viruensis–P. robustus* assemblage established in the study area corresponds to the upper part of the *P. originalis* to *P. serra* zone in the Jiangnan Slope region and the *L. antivariabilis* to *P. serra* zone in the Yangtze platform region, which corresponds to the *H. holodentata–T. tangshanensis* to the *P. serra* zone in the North China Block, the *M. parva* to the *P. serra* zone in the Tarim Block, and the *L. variabilis* to the *P. serra* zone in the Qinling Block (Table 1). This conodont zone mainly contains *S. rex* and *P. parallelus*.

5.2 Evolution of conodont biota in the study area

The earliest euconodonts that appeared in the Furongian are single forms dominated by simple cone elements. At this time, there was no zoning phenomenon evident in the conodont fauna at a global scale (Dong et al., 2004; Dong and Zhang, 2017; Bagnoli et al., 2017). During the Ordovician, the global conodont biogeographic region can be divided into the North Atlantic Province and the North American Midcontinent Province (Sweet, 1979, 1984). The North Atlantic Province type yields cold-water elements that mainly developed in cold deep-water environments at higher latitudes, while the North American Midcontinent Province type yields warm-water elements that mainly developed in warm shallow-water environments at lower latitudes (Bergström and Sweet, 1966; Zhen and Percival, 2003; Barnes, 2020). In addition, the transitional type that mixed with North Atlantic Province type and North American Midcontinent Province type was often observed at the margin of some blocks, such as the eastern margin of North America adjacent to the Appalachian belt (Sweet, 1979, 1984), the western margin of the North China Block (An and Zheng, 1990), the Qinling Block (Pei, 2000), and the perimeter of the Tarim Block (Jing, 2009; Jing et al., 2012). However, the reasons controlling the evolution of the conodont biogeographic region and the mixing of elements from different types remain controversial (Sweet and Bergström, 1972; Wang et al., 1996; Pei, 2000; Barnes, 2020).

The six conodont zones (*C. proavus*, *C. lindstromi*, *I. fluctivagus*, *C. angulatus*, *R. manitouensis*, and *C. quadraplicatus*) from the Stage 10 to the middle part of the Tremadocian in the Chuzhou area belong to the North American Midcontinent Province (warm-water biota) (Lindström, 1971; Dong et al., 1987). The three conodont zones (*P. deltifer*, *P. proteus*, and *T. bifidus*) and the three assemblages (*J. anhuiensis–P. gradates*, *N. giganteus–P. parallelus*, and *D. viruensis–P. robustus*) from the upper part of the Tremadocian to the Darriwilian belong to the North Atlantic Province (cold-water biota) (Table 2). This suggests that the transition of conodont biota in the Chuzhou area occurred in the middle Tremadocian, slightly earlier than the start of the South China Block, and contemporaneous with the Qinling Block, Tarim Block, and North China Block (Table 2).

5.3 Causes and paleogeographic implications of the conodont biogeographic region

Various theories have been proposed to explain the transitions of the conodont biogeographic region and the emergence of mixed species. Sweet and Bergström (1972) suggested that the changes in water temperature related to the latitudinal shifts controlled the formation of the conodont biogeographic region. The mixing of cold-water biota and warm-water biota mainly occurred in the mid-latitudes, sandwiched between the North American Midcontinent Province type area and the North Atlantic Province type area. An (1981) proposed that the flooding of seawater from trough areas into the interior of blocks led to the transformation of conodonts from the North Atlantic Province type conodonts (deep water and cold water) to the North American Midcontinent type (shallow water and warm water). Pei (2000) argued that the rapid movement of blocks drove the evolution of the conodont biogeographic region. Wang et al. (2016) suggested that the development of the Ordovician conodont fauna was linked to depositional environments, with changes in the water depth and temperature resulting in the transition of the conodont biogeographic region. Jing (2009) and Jing et al. (2012) pointed out that the transition of conodont biogeographic regions was related to a combination effect of block movement and ocean currents. In this study, we conducted a comprehensive analysis of block movement, sea level change, current affairs, and climatic fluctuation to understand the transition of the conodont biogeographic region in the Chuzhou area.

During the Early Ordovician, the South China Block was situated at approximately 30° S and then shifted northward to around the Equator by the Middle Ordovician (Fig. 8) (Cocks and Torsvik, 2013). Generally, block movements from high latitude to low latitude can increase the surrounding seawater's temperature and promote the development of warm-water biota. However, the transition of the conodont biogeographic region in the Chuzhou area shows an opposite trend (Table 2), suggesting that block movements had limited influence on the change in the conodont biogeographic region in the study area.

Table 2. Comparison of the conodont biogeographic regions of the Chuzhou area with the North Atlantic Province (Lindström, 1971), North American Midcontinent Province (Sweet, 1984), South China (Wang et al., 2019), Qinling (Pei, 2000), Tarim (Jing, 2009), and North China (Wang et al., 2014).

Series	Stage	North Atlantic Province	North American Province	South China	Chuzhou (this study)	Qinling	Tarim	North China
				Yangtze platform				
Middle Ordovician	Darriwilian	*P. serra*	*Cahabagnathus sweeti*	*P. serra*	*D. variabilis–P. robustus* (assemblage)	*P. serra*	*P. serra*	*P. serra*
			C. friendsvillensis					*P. anitae*
		E. suecicus	*Phragmodus* "pre-flexuosus"	*E. suecicus*		*E. suecicus*	*E. suecicus*	*E. suecicus*
			Histiodella holodentata	*E. pseudoplanus–D. tablepointensis*			*Y. crassus*	*H. holodentata–T. tangshanensis*
		A. variabilis	*H. sinuosa*	*Y. crassus*				
		M. parva	*H. altifrons*	*L. variabilis*		*L. variabilis*	*L. variabilis*	
			M. flabellum–T. laevis	*L. antivariabilis*			*M. parva*	
	Dapingian	*P. originalis–B. navis*	*P. aranda–J. jaanussoni*	*M. parva*	*N. giganteus–P.parallelus* (assemblage)	*P. orginalis*	*A. iaptosomatus–L. dissectus*	
				P. orginalis				
		B. triangularis	*J. gananda–R. andinus*	*B. navis*			*S. chuxianensis–S. euspinus*	
			B. communis	*B. triangularis*				
Lower Ordovician	Floian	*O. evae*	*A. deltatus–M. dianae*	*O. communis/O. evae*		*O. evae*	*S. diversus–S. tarimensis–P. proteus*	*J. gananda*
				P. honghuayuanensis	*J. anhuiensis–P. gradates* (assemblage)			*P. obesus*
								S. extensus
		P. elegans		*S. diversus*		*P. elegans*		*S. bilobatus*
	Tremadocian	*P. proteus*		*T. bifidus*	*T. bifidus*	*P. proteus*	*T. proteus–P. deltifer*	*S. tersus–T.bifidus*
				T. proteus–C. quadraplicatus	*P. proteus*			
					P. deltifer	*P. deltifer*		
					C. quadraplicatus		*G. floweri*	*C. quadraplicatus*
			Low-diversity interval				*C. quadraplicatus*	
		? *C. angulatus*	*G. quadraplicatus–S. rex*	*R. manitouensis*			*C. herfurthi–R. manitouensis*	*C. herfurthi–R. manitouensis*
				C. angulatus	*C. angulatus*	*C. angulatus*		
							T. nakamurai–T. huanghuachang–T.gracilis	*I. jilinensis*
Furongian	Stage 10		*I. fluctivagus*	*M. sevierensis*	*I. fluctivagus*			
			C. lindstromi		*C. lindstromi*			*C. lindstromi*
				C. proavus	*C. proavus*			*C. proavus*
			C. intermedius					

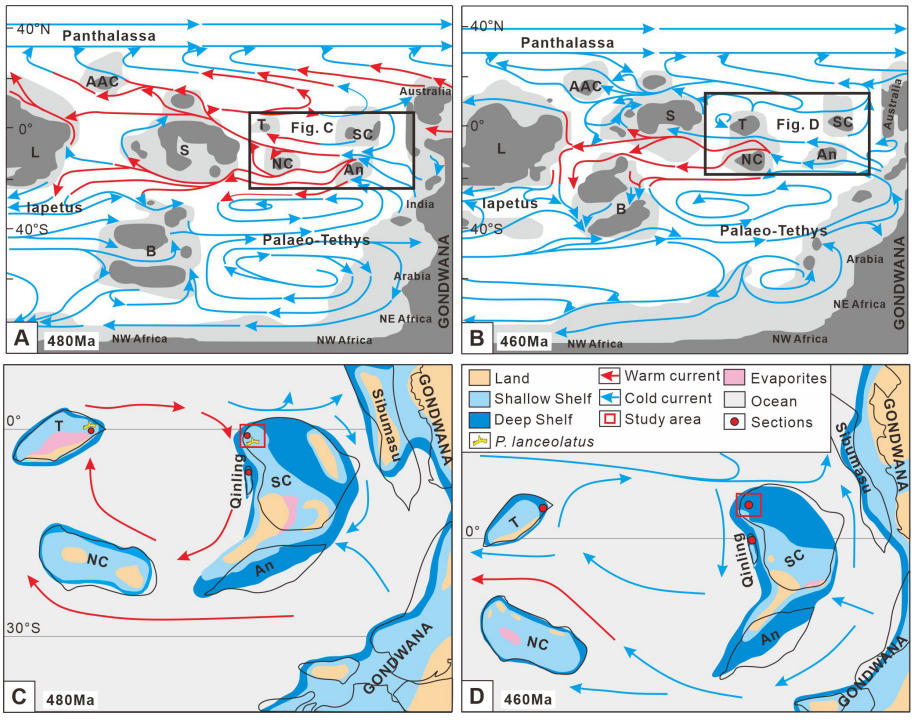

Figure 8. **(a)** Early Ordovician (480 Ma) synthetic ocean surface circulation. **(b)** Middle Ordovician (460 Ma) synthetic ocean surface circulation, modified from Pohl et al. (2016). **(c)** Early Ordovician ocean current model of the South China Block. **(d)** Middle Ordovician ocean current model of the South China Block, modified from Cocks and Torsvik (2013) and Dong et al. (2021). L is for Laurentia, B is for Baltica, S is for Siberia, A is for Avalonia, AAC is for Arctic Alaska Chukotka, An is for Annamia, NC is for North China, SC is for South China, and T is for Tarim.

The study area, located on the margin of the Yangtze platform, has significant responses to sea level fluctuations and biota changes (Luan et al., 2018, 2021). The Furongian Stage 10 Cheshuitong Formation, consisting of thick-bedded limestone and dolomitic limestone, suggests deposition in a shallow-seawater environment. Conodonts produced in this formation were small with species characterized by simple cone mainly composited of the Cambrian elements that flourished in the Ordovician. The early Tremadocian Shangouchong Formation, composed of lime mudstone and dolomitic limestone and deposited in a shallow-water platform, produced an increasing number of conodonts belonging to warm-water fauna. The late Tremadocian Fenxiang Formation mainly comprises peloid packstone with minor shale, indicating a slight deepening of seawater in the study area. Conodonts in this formation are dominated by warm-water fauna with minor cold-water fauna. From the Floian to the Darriwilian, the Honghuayuan, Dawan, and Kuniutan formations predominantly consist of bioclastic limestone, nodular limestone, calcarenite, and micritic limestone, respectively. This suggests a rising sea level trend, resulting in a gradual decrease in seawater temperature. Consequently, elements of the cold-water type developed, and the conodont biogeographic region gradually transformed into the North Atlantic Province.

The evolution of Ordovician conodonts in the Lower Yangtze region indicates that three diversity peak events occurred in the late Tremadocian to early Floian (*S. diffusus* zone), early Dapingian (*B. triangularis* and *B. navis* zone), and middle to late Darriwilian (*E. suecicus* zone), respectively, corresponding to three sea-level-rise episodes (Liu, 2006; Su, 2007; Wu and Wang, 2008; Wu et al., 2008; Wang and Wu, 2009). Particularly, the first diversity event (Wang and Wu, 2009; Wu et al., 2014) that happened during the late Tremadocian to early Floian (*S. divers* zone) was the most significant diversity peak of the Ordovician with corresponding conodont zones of *P. deltifer*, *P. proteus*, and *T. bifidus* and the *J. Anhuiensis–P. gradates* assemblage. These four conodont zones (or assemblages) belonging to the North Atlantic Province also appeared in the Jiangnan Slope type conodont biostratigraphy, indicating that seawater in the study area became deeper during this period and more suitable for developing cold-water fauna. This sea level change may have influenced the transition of the conodont biogeographic region in the study area from the North American Midcontinent Province to the North Atlantic Province. Additionally, the climate cooling event during the Early to Middle Ordovician (Trotter et al., 2008; Fang et al., 2019; Samuel et al., 2021) may have promoted this transition.

Furthermore, the Chuzhou area on the northeastern margin of the Lower Yangtze region connects the South China Block, the North China Block, and the Qinling–Dabie orogenic belt, facilitating seawater exchange among these blocks and promoting biodiversity (Zhu et al., 1984). Other paleontological communities in the Chuzhou area also exhibit differences from the interior of the South China Block during the Furongian–Middle Ordovician, apart from the transition of the conodont biota (Lu, 1975; Lu et al., 1976; Lu and Zhu, 1980; Anhui Provincial Geological Survey, 1987).

Ocean surface circulation may play a vital role in the migration and evolution of conodonts, which can have different effects on the regional environment. A clockwise surface ocean circulation among the Tarim, South China, Qinling, and North China blocks from the end of the Furongian to the Early Ordovician was characterized by warm currents (Pohl et al., 2016) (Fig. 8a, c). The warm current increased the seawater temperature in the surrounding areas, marking it suitable for developing warm-water species (Barnes and Fåhræus, 1975; Barnes, 2020). Conodonts in these blocks were dominated by the North American Midcontinent Province type. Since the Middle Ordovician, the nature of ocean currents has changed from warm to cold (Pohl et al., 2016) (Fig. 8b, d), decreasing the seawater temperature and favoring the flourishing of cold-water fauna. Conodonts in the South China, Tarim, and Qinling blocks began to transform from the North American Midcontinent Province to the North Atlantic Province.

Moreover, several crucial conodont elements with particular paleogeographic importance were also found in the Ordovician strata in the Chuzhou area. For example, the *I. fluctivagus* zone, defined as the lower boundary of the Ordovician, was first reported from the Lower Yangtze Block, enriching the global distribution of the conodont zone. *Parapanderodus lanceolatus* was found in the lower part of the Shangouchong Formation, previously reported from only from the Lower Ordovician Qulitage Subgroup of the Tarim Block (Zhao and Tan, 1999). This suggest that the Lower Yangtze region and Tarim Block were adjacent to each other during the Early Ordovician, allowing for conodont migration through oceanic currents (Fig. 8c). Thus, the study area served as an important connection point between different blocks, potentially recording global biota characteristics and paleoceanographic characteristics, making it an ideal area to study the co-evolution of Cambrian–Ordovician organisms and environments.

6 Conclusions

The study identified 28 genera and 45 species of conodonts, establishing nine conodont zones, including *Cordylodus proavus*, *Cordylodus lindstromi*, *Iapetoganathus fluctivagus*, *Cordylodus angulatus*, *Rossodus manitouensis*, *Colaptoconus quadraplicatus*, *Paltodus deltifer*, *Paroistodus proteus*, *Triangulodus bifidus*, and three assemblages, including *Juanognathus anhuiensis–Protopanderodus gradates*, *Nasusgnathus giganteus–Paroistodus parallelus*, and *Dapsilodus viruensis–Protopanderodus robustus*.

The conodont biogeographic region in the Chuzhou area from Stage 10 to the middle Tremadocian belongs to the North American Midcontinent Province type, while from the late Tremadocian to the Darriwilian, it belongs to the North Atlantic Province type. This transition in conodont biogeography may be related to the sea level changes and ocean currents associated with the paleogeography of the study area.

The discovery of the *Iapetognathus fluctivagus* zone and the element *Parapanderodus lanceolatus* in the Lower Yangtze region enriches the global paleogeographic distribution of these species and suggests the existence of seawater connections among different blocks.

Code and data availability. All data, models, and code generated or used during the study appear in the submitted article. Conodont data are available in the Supplement.

Supplement. The supplement related to this article is available online at: https://doi.org/10.5194/jm-43-283-2024-supplement.

Author contributions. SL came up with the concept for this study. BH, ML, WX, and WX did the fieldwork. BH did the conodont work and analyzed the data. BH wrote the paper with revisions by SL and CC.

Competing interests. The contact author has declared that none of the authors has any competing interests.

Disclaimer. Publisher's note: Copernicus Publications remains neutral with regard to jurisdictional claims made in the text, published maps, institutional affiliations, or any other geographical representation in this paper. While Copernicus Publications makes every effort to include appropriate place names, the final responsibility lies with the authors.

Acknowledgements. The authors sincerely appreciate Zhihao Wang from the Nanjing Institute of Geology and Palaeontology, Chinese Academy of Sciences, for his help in identifying conodont fossils. We thank Bo Li and Jian Jiang for their help during the fieldwork. The authors extend their special thanks to associates Zhensheng Li and Yuefeng Shen for their helpful discussions. During the writing process of this article, ChatGPT3.5 was used to polish some sentences. The authors would like to express their gratitude for this.

Financial support. This research has been supported by the National Natural Science Foundation (grant nos. 41772098 and 42002111) and the Public Welfare Geological Work Project of Anhui Province ("Investigation and evaluation of energy resources in basins around the Tanlu fault zone (Anhui section)") (grant no. 2015-g-24).

Review statement. This paper was edited by Luke Mander and reviewed by Tonn Paiste and one anonymous referee.

References

Albanesi, G. L., Giuliano, M. E., Pacheco, F. E., Ortega, G., and Monaldi, C. R.: The Cambrian-Ordovician boundary in the Cordillera Oriental, NW Argentina, Stratigraphy, 12, 19–21, https//doi.org/10.2110/sepmord.015, 2015.

An, T. X.: Recent progress in Cambrian and Ordovician conodont biostratigraphy of China, Geology Society of America, 187, 209–236, https//doi.org/10.1130/spe187-p209, 1981.

An, T. X. (Ed.): Early Paleozoic conodonts in southern China, Peking University Press, Beijing, China, 238 pp., ISBN13209.145, 1987 (in Chinese).

An, T. X. and Zheng, Z. C. (Eds.): Conodonts in the periphery of Ordos Basin, Science Press, Beijing, China, 193 pp., ISBN7030017161, 1990 (in Chinese).

An, T. X., Zhang, F., Xiang,W. D., Zhang, Y. Q., Xu,W. H., Zhang, H. J., Jiang, D. B., Yang, C. S., Lin, L. D., Cui, Z. T., and Yang, X. C. (Eds.): The Conodonts of North China and the Adjacent Regions, Science Press, Beijing, China, 223 pp., ISBN130312295, 1983 (in Chinese with English abstract).

Anhui Provincial Bureau of Geology and Mineral Resources (Ed.): Regional Geology of Anhui Province, Geological Press, Beijing, China, 270 pp., ISBN13038.206, 1987 (in Chinese).

Bagnoli, G., Peng, S. C., Qi, Y. P., and Wang, C. Y.: Conodonts from the Wa'ergang section, China: A potential GSSP for the uppermost stage of the Cambrian, Riv. Ital. Paleontol. S., 123, 1–10, https//doi.org/10.13130/2039-4942/8003, 2017.

Barnes, C. R.: The proposed Cambrian-Ordovician global boundary stratotype and point (GSSP) in western Newfoundland, Canada, Geol. Mag., 125, 381–414, https://doi.org/10.1017/S0016756800013042, 1988.

Barnes, C. R.: Impacts of climate-ocean-tectonic changes on early Paleozoic conodont ecology and evolution evidenced by the Canadian part of Laurentia, Palaeogeogr. Palaeocl., 549, 109092, https://doi.org/10.1016/j.palaeo.2019.02.018, 2020.

Barnes, C. R. and Fåhræus, L. E.: Provinces, communities, and the proposed nektobenthic habit of Ordovician conodontophorids, Lethaia, 8, 133–149, https//doi.org/10.1111/j.1502-3931.1975.tb01308.x, 1975.

Bergström, S. M. and Ferretti, A.: Conodonts in Ordovician biostratigraphy, Lethaia, 50, 424–439, https//-doi.org/10.1111/let.12191, 2017.

Bergström, S. M. and Sweet, W. C.: Conodonts from the Lexington Limestone (Middle Ordovician) of Kentucky, and its lateral equivalents in Ohio and Indiana, Bulletin of American Paleontology, 50, 271–441, 1966.

Berner, R. A.: Modeling atmospheric O_2 over Phanerozoic, Geochim. Cosmochim. Ac., 65, 685–694, https//doi.org/10.1016/S0016-7037(00)00572-X, 2001.

Branson, E. B. and Mehl, M. G.: Conodont studies, Univsity of Missouri Studies, 8, 1–349, 1933.

Chen, J.: Aspects of Cambrian-Ordovician boundary in Dayangcha, China, Geologiska Föreningen i Stockholm Förhandlingar, 110, 2, 120, https://doi.org/10.1080/11035898809452650, 1988.

Cocks, L. and Torsvik, T. H.: The dynamic evolution of the Palaeozoic geography of eastern Asia, Earth-Sci. Rev., 117, 40–79, https//doi.org/10.1016/j.earscirev.2012.12.001, 2013.

Cooper, R. A., Nowlan, G. S., and Williams, S. H.: Global stratotype section and point for base of the Ordovician System, Episodes Journal of International Geoscience, 24, 19–28, https://doi.org/10.18814/epiiugs/2001/v24i1/005, 2001.

Ding, L. S.: Ordovician conodont biostratigraphy and lithofacies paleogeography, in: Conodonts in the Lower Yangtze Region, Indicators of Maturity of Biostratigraphic and Organic Systems, edited by: Wang, C., Science Press, Beijing, China, 16–31, ISBN7030034627, 1993 (in Chinese).

Dong, X. P.: Late Cambrian to Early Ordovician conodonts in Chuzhou, Anhui, Graduate Thesis Collection of Nanjing Institute of Geology and Palaeontology, Chinese Academy of Sciences, 1, 83–111, 1987 (in Chinese with English abstract).

Dong, X. P.: A potential candidate for the Middle-Upper Cambrian boundary stratotype-An introduction to the Paibi Section in Huayuan, Hunan, Acta Geol. Sin.-Engl., 01, 62–79, 94–97, 1990 (in Chinese with English abstract).

Dong, X. P.: Cambrian conodont sequences in South China, Chinese Science Part D: Earth Science, 04, 339–346, 1999 (in Chinese).

Dong, X. P. and Zhang, H. Q.: Middle Cambrian through lowermost Ordovician conodonts from Hunan, South China, J. Paleontol., 91, 1–89, https//doi.org/10.1017/jpa.2015.43, 2017.

Dong, X. P., Repetski, J. E., and Bergström, S. M.: Conodont biostratigraphy of the Middle Cambrian through Lowermost Ordovician in Hunan, South China, Acta Geol. Sin.-Engl., 78, 1185–1206, https//doi.org/10.1111/j.1755-6724.2004.tb00776.x, 2004.

Dong, Y., Sun, S., Santosh, M., Zhao, J., Sun, J., He, D., Shi, X., Hui, B., Cheng, C., and Zhang, G.: Central China Orogenic Belt and amalgamation of East Asian continents, Gondwana Res., 100, 131–194, https://doi.org/10.1016/j.gr.2021.03.006, 2021.

Druce, E. C. and Jones, P. J.: Cambro-Ordovician conodonts from the Burke River structural belt, Queensland, Bulletin of the Bureau of Mineral Resources, Geology and Geophysics, 110, 1–159, 1971.

Dzik, J.: Remarks on the evolution of Ordovician conodonts, Acta Paleontology Polonica, 21, 395–57, 1976.

Fang, Q., Wu, H. C., Wang, X. L., Yang, T. S., Li, H. Y., and Zhang, S. H.: An astronomically forced cooling event during the Middle Ordovician, Global Planet. Change, 173, 96–108, https//-doi.org/10.1016/j.gloplacha.2018.12.010, 2019.

Feng, Z. Z., Peng, Y. M., Jin, Z. K., Jiang, P. L., Bao, Z. D., Tian, H. Q., Wang, H., Luo, Z., and Ju, T. Y.: Lithofacies palaeogeography of the middle and Late Ordovician in South China, J. Palaeogeogr., 002, 11–22, 2001 (in Chinese with English abstract).

Feng, Z. Z., Peng, Y. M., Jin, Z. K., and Bao, Z. D.: Lithofacies palaeogeography of the middle Ordovician in China, J. Palaeogeogr., 03, 263–278, 2003 (in Chinese with English abstract).

Furnish, W. M.: Conodonts from the Prairie du Chien (Lower Ordovician) beds of upper Mississippi Valley, J. Paleontol., 12, 318–340, 1938.

Gong, Y. F., Yan, G. Z., and Wu, R. C.: Conodont biostratigraphy and carbon isotope chemostratigraphy of the Middle to Upper Ordovician on the western Yangtze Platform, South China, Palaeoworld, 32, 266–286, https//doi.org/10.1016/j.palwor.2022.01.005, 2023.

Graves, R. W. and Ellison S. P.: Ordovician conodonts of the Marathon Basin, Texas, University of Missouri School of Mining and Metallurgy Bulletin Technical, 14, 1–16, 1941.

Hadding, A.: Undre Dicellograptus akiffern? Skane Jamte Nagre Darmet Ekivalenta Bildinger, Lunds Univsity, 9, 1–90, 1913.

Haq, B. U. and Schutter, S. R.: A chronology of Paleozoic sea-level changes, Science, 322, 64–68, https//-doi.org/10.1126/science.1161648, 2008.

Harper, D. A. T., Topper, T. P., Cascales-Miñana, B., Servais, T., Zhang, Y. D., and Ahlber, P.: The Furongian (late Cambrian) Biodiversity Gap: Real or apparent?, Palaeoworld, 28, 4–12, https//-doi.org/10.1016/j.palwor.2019.01.007, 2019.

Henningsmoen, G.: The Tretaspis series of the Kullatorp core, Bulletin of the Geological Institute of the University of Uppsala, 32, 374–432, 1948.

Jeppsson, L., Anehus, R., and Fredholm, D.: The optimal acetate buffered acetic acid technique for extracting phosphatic fossils, J. Paleontol., 73, 964–972, https://doi.org/10.1017/S0022336000040798, 1999.

Ji, Z. and Barnes, C. R.: Conodont paleoecology of the Lower Ordovician St. George Group, Port au Port Peninsula, western Newfoundland, J. Paleontol., 68, 1368–1393, https//-doi.org/10.1017/S002233600003434x, 1994.

Jing, X. C.: The Ordovician conodonts and the Cambrian-Ordovician boundary at the platform facies in the Tarim Basin, China, Ph.D. thesis, China University of Geosciences, China, 156 pp., 2009 (in Chinese with English abstract).

Jing, X. C., Deng, S. H., Wang, X. L., and Zhang, S. B.: Biota attribution and transformation of conodonts in Ordovician platform facies area of Tarim Basin, Sciencepaper Online, 201205, 432, https://www.paper.edu.cn/releasepaper/content/201205-432 (last accessed: 30 July 2024), 2012 (in Chinese with English abstract).

Jing, X. C., Zhou, H. R., and Wang, X. L.: Ordovician (middle Darriwilian-earlist Sandbian) conodonts from the Wuhai area of Inner Mongolia, North China, J. Paleontol., 89, 768–790, https//-doi.org/10.1017/jpa.2015.54, 2015.

Jing, X. C., Stouge, S., Ding, L., Wang, X. L., and Zhou, H. R.: Upper Ordovician conodont biostratigraphy and biofacies from the Sigang secton, Neixiang, Henan, central China, Palaeogeogr. Palaeocl., 480, 18–32, https//-doi.org/10.1016/j.palaeo.2017.04.026, 2017.

Li, S. Y., Xie, W., Wei, X., Yang, D. D., Li, M., and Hu, B.: Discovery of the mid-Cretaceous sedimentary rocks from the ultrahigh-pressure terrane, Dabie Orogenic Belt, and its tectonopalaeogeographic implications, J. Palaeogeogr., 12, 1, 153–177, https://doi.org/10.1016/j.jop.2023.01.001, 2023.

Lindström, M.: Conodonts from the lowermost Ordovician strata of south-central Sweden, Geologiska Föreningens i Stockholm Förhandlingar, 76, 517–604, https//-doi.org/10.1080/11035895409453581, 1955.

Lindström, M.: Lower Ordovician conodonts of Europe, Geol. Soc. Am. Mem., 127, 21–62, https//doi.org/10.1130/mem127-p21, 1971.

Lindström, M.: Baltoscandic conodont life environments in the Ordovician: sedimentologic and palaeogeographic evidence, in: Conodont Biofacies and Provincialism, edited by: Clark, D. L., Geological Society of America Special Paper, 196, 33–42, https://doi.org/10.1130/SPE196-p33, 1984.

Liu, J.: Marine sedimentary response to the great Ordovician biodiversification event: Examples from North China and South China, Paleontol. Res., 13, 9–21, https://doi.org/10.2517/1342-8144-13.1.009, 2009.

Liu, J., Zhan, R., Dai, X., Liao, H., Ezaki, Y., and Adachi, N.: Demise of Early Ordovician oolites in South China: Evidence for paleoceanographic changes before the GOBE, Ordovician of the World, Cuadernos del Museo Geominero, 14, 309–317, 2011.

Liu, J. B.: Sea level changes during the early to middle Ordovician biological radiation in South China, in: Originations, Radiations and Biodiversity Changes-Evidences from the Chinese Fossil Record, edited by: Rong, J. Y., Fang, Z. J., Zhou, Z. H., Zhan, R. B., Wang, X. D., and Yuan, X. L., Science Press, Beijing, China, 335–360, ISBN7030174410, 2006 (in Chinese).

Lu, Y. H. (Ed.): Ordovician trilobite fauna from central and southwest China, Science Press, Beijing, China, 463 pp., ISBN 13031257, 1975 (in Chinese).

Lu, Y. H. and Zhu, Z. L.: Cambrian trilobites from Chuxian and Quanjiao, Anhui, Journal of Nanjing Institute of Geology and Palaeontology, Chinese Academy of Sciences, 16, 1–38, 1980 (in Chinese).

Lu, Y. H., Qian, Y. Y., and Zhou, Z. Y.: Ordovician biostratigraphy and palaeozoogeography in China, Journal of Nanjing Institute of Geology and Palaeontology, Chinese Academy of Sciences, 7, 1–90, 1976 (in Chinese).

Luan, X., Brett, C. E., Zhan R., Jin, J. Wu, R., and Gong, F.: Middle-Late Ordovician iron-rich nodules on Yangtze Platform, South China, and their palaeoenvironmental implications, Lethaia, 51, 523–537, https://doi.org/10.1111/let.12271, 2018.

Luan, X., Zhang, X., Wu, R., Zhan, R., Liu, J., Wang, G., and Zhang, Y.: Environmental changes revealed by Lower-Middle Ordovician deeper-water marine red beds from the marginal Yangtze Platform, South China: Links to biodiversification, Palaeogeogr. Palaeocl., 562, 110116, https://doi.org/10.1016/j.palaeo.2020.110116, 2021.

Luan, X. C., Wu, R. C., Zhan, R. B., and Liu J. B.: The Zitai Formation in South China: unique deeper-water marine red beds in terms of lithology, distribution and $\delta^{13}C_{carb}$ chemostratigraphy, Palaeoworld, 28, 198–210, https://doi.org/10.1016/j.palwor.2018.12.007, 2019.

Miller, A. I.: Ordovician Radiation, in: Palaeobiology II, edited by: Briggs, D. E. G. and Crowther, P. R., Blackwell Publishing, Oxford, 49–52, https://doi.org/10.1002/9780470999295.ch9, 2003.

Miller, J. F.: Conodont fauna of the Notch Peak Limestone (Cambro-Ordovician), House Range, Utah, J. Paleontol., 43, 413–439, https//doi.org/10.2307/1302317, 1969.

Miller, J. F.: Upper Cambrian to Middle Ordovician Conodont Faunas of Western Utah, Southwest Missouri State University, Department of Geography and Geology, 1978.

Miller, J. F.: Taxonomic revisions of some Upper Cambrian and Lower Ordovician conodonts with comments on their evolution,

The University of Kansas Paleontological Contributions, 99, 1–40, http://hdl.handle.net/1808/3732 (last accessed: 30 July 2024), 1980.

Miller, J. F., Repetski, J. E., Nicoll, R. S., Nowlan, G., and Ethington, R. L.: The conodont Iapetognathus and its value for defining the base of the Ordovician System, GFF, 136, 185–188, https//-doi.org/10.1080/11035897.2013.862851, 2014.

Miller, J. F., Evans, K. R., Ethington, R. L., Freeman, R. L., Loch, J. D., Repetski, J. E., Ripperdan, R. L., and Taylor, J. F.: Proposed auxiliary boundary stratigraphic section and point (ASSP) for the base of the Ordovician System at Lawson Cove, Utah, USA, Stratigraphy, 12, 219–236, 2015.

Moskalenko, T. A.: Conodonts of the Chunk Stage (Middle Ordovician). River Moiera and Podkamennaya Tunguska, In New data on the biostratigraphy of the Lower Palezoics of the Siberian Platform, Izdatelstvo "Nauka", 98–116, 1967.

Müller, K. J.: Kambrisch conodonten, Zeitschrift der Deutschen Geologischen Gesellschaft, 111, 434–485, 1959.

Munnecke, A., Zhang, Y. D., Liu, X., and Cheng, J. F.: Stable carbon isotope stratigraphy in the Ordovician of South China, Palaeogeogr. Palaeocl., 307, 17–43, https//-doi.org/10.1016/j.palaeo.2011.04.015, 2011.

Ni, S. Z.: Discusses several stratigraphic issues from the Ordovician conodonts in the eastern Three Gorges region, in: the first academic symposium of the Chinese Society of micropalaeontology, Science Press, Beijing, 121–126, 1981 (in Chinese).

Ni, S. Z. and Li, Z. H.: Conodont, Biostratigraphy in the Three Gorges area of the Yangtze River (2), Early Paleozoic Volume, edited by: Yichang Institute of Geology and Mineral Resources, Geological Publishing House, Beijing, China, 386–448, ISBN 13038.352, 1987 (in Chinese).

Nicoll, R. S., Miller, J. F., Nowlan, G. S., Repetski, J. E., and Ethington, R. L.: Iapetonudus (N. gen.) and Iapetognathus Landing, unusual earliest Ordovician multielement conodont taxa and their utility for biostratigraphy, Brigham Young University Geology Studies, 44, 27–55, 1999.

Nogami, Y.: Kambrischen condonten von China, Teil 2, Conodonten aus den hoch oberkambrischen Yencho-Schichten, Kyoto University, 33, 211–219, http://hdl.handle.net/2433/258338 (last accessed: 30 July 2024), 1967.

Pander, C. H.: Monographie der fossilen Fische des Silurchen Systems der russischen Gouvernements, Buchdruckerei der Kaiserlichen Akademie der Wissenschaften, St. Petersburg, 91, 1856.

Pei, F.: Qinling faunal region-The third Ordovician faunal region: international correlation, Acta Geol. Sin.-Engl., 74, 137–142, https//doi.org/10.1111/j.1755-6724.2000.tb00441.x, 2000.

Pohl, A., Nardin, E., Vandenbroucke, T. R. A., and Donnandieu, Y.: High dependence of Ordovician ocean surface circulation on atmospheric CO_2 levels, Palaeogeogr. Palaeocl., 458, 39–51, https://doi.org/10.1016/j.palaeo.2015.09.036, 2016.

Pyle, L. J. and Barnes, C. R.: Conodonts from the Kechika Formation and Road River Group (Lower to Upper Ordovician) of the Cassiar Terrane, northern British Columbia, Can. J. Earth Sci., 38, 1387–1401, https://doi.org/10.1139/e01-033, 2001.

Repetski, J. E. and Ethington, R. L.: *Rossodus manitouensis* (Conodonta), A new early Ordovician index fossil, J. Paleontol., 57, 289–301, 1983.

Samuel, L. G., Theodore M. P., Seth, F., and Kristin D. B.: A high-resolution record of early Paleozoic climate, P. Natl. Acad. Sci. USA, 118, e2013083118, https//-doi.org/10.1073/pnas.2013083118, 2021.

Schmitz, B., Bergström, S. M., and Wang, X. F.: The middle Darriwilian (Ordovician) $\delta^{13}C$ excursion (MDICE) discovered in the Yangtze Platform succession in China: Implications of its first recorded oc-currences outside Baltoscandia, J. Geol. Soc., 167, 249–259, https//doi.org/10.1144/0016-76492009-080, 2010.

Seddon, G. and Sweet, W. C.: An ecologic model for conodonts, J. Paleontol., 45, 869–880, 1971.

Sepkoski, J. J.: A kinetic model of Phanerozoic taxonomic diversity I: Analysis of marine orders, Paleobiology, 4, 223–251, https//-doi.org/10.1017/ S0094837300005972, 1978.

Sepkoski, J. J.: A kinetic model of Phanerozoic taxonomic diversity II: Early Phanerozoic families and multiple equilibria, Paleobiology, 5, 222–252, https//doi.org/10.1017/S0094837300006539, 1979.

Sepkoski, J. J.: A factor analytic description of the Phanerozoic marine fossil record, Paleobiology, 7, 36–53, https//-doi.org/10.2307/2400639, 1981.

Sepkoski, J. J.: A kinetic model of Phanerozoic taxonomic diversity III: Post Paleozoic families and mass extinctions, Paleobiology, 10, 246–267, https//doi.org/10.1017/S0094837300008186, 1984.

Sepkoski, J. J.: The Ordovician Radiations: diversification and extinction shown by global genus-level taxonomic data, in: Ordovician Odyssey: Short Papers for the Seventh International Symposium on the Ordovician System, edited by: Cooper, J. D., Droser, M. L., and Finney, S. C., SEPM, California, 393–396, 1995.

Sepkoski, J. J. and Sheehan, P. M.: Diversification, faunal change, and community replacement during the Ordovician Radiations, in: Biotic Interactions in Recent and Fossil Benthic Communities, edited by: Tevesz, M. J. S. and McCall, P. L., Plenum Press, New York, 673–717, https://doi.org/10.1007/978-1-4757-0740-3_14, 1983.

Sergeeva, S. P.: Novyy ranneordovikskiy rod konodontov semeystva Prioniodinidae (A new Early Ordovician conodont genus of the family Prionidinidae), Paleontology, 4, 138–140, 1963.

Serpagli, E.: Lower Ordovician conodonts from western Precordilleran Argentina (Province of San Juan), Bolletttino della Societa Paleontologica Italiana, 13, 17–98, 1974.

Su, W. B.: Ordovician sea-level changes: evidence from the Yangtze Platform, Acta Palaeontologica Sinica, 46, 471–476, 2007 (in Chinese with English abstract).

Sweet, W. C.: Late Ordovician conodonts and biostratigraphy of the Western Midcontinent Province, Brigham Young University Geology Studies, 26, 45–86, 1979.

Sweet, W. C.: Graphic correlation of upper Middle and Upper Ordovician rocks, North American Midcontinent Province, USA, in: Aspects of the Ordovician System, edited by: Bruton, D. L., Paleontological Contributions of the University of Oslo, 295, 23–35, 1984.

Sweet, W. C. and Bergström, S. M.: Conodonts from the Pratt Ferry Formation (Middle Ordovician) of Alabama, J. Paleontol., 36, 1214–1252, https//doi.org/10.2307/1301327, 1962.

Sweet, W. C. and Bergström, S. M.: Multielement taxonomy and Ordovician conodonts, Geologica et Palaeontologica, Special Paper, 1, 29–42, 1972.

Sweet, W. C. and Bergström, S. M.: Conodont provinces and biofacies of the Late Ordovician, Special Paper of the Geological

Society of America, 196, 69–88, https//doi.org/10.1130/spe196-p69, 1984.

Torsvik, T. H. and Cocks, L. R. M.: New global palaeogeographical reconstructions for the Early Palaeozoic and their generation, Geological Society London Memoris, 38, 5–24, https//-doi.org/10.1144/M38.2, 2013.

Trotter, J. A., Williams, I. S., Barnes, C. R., Lécuyer, C., and Nicoll, R. S.: Did cooling oceans trigger Ordovician biodiversification? Evidence from conodont thermometry, Science, 321, 550–554, https//doi.org/10.1126/ science.1155814, 2008.

Wang, C. Y. (Ed.): Conodonts in the Lower Yangtze Region: Indicators of Maturity of Biostratigraphic and Organic Systems, Science Press, Beijing, China, 326 pp., ISBN 7030034627, 1993 (in Chinese).

Wang, G. X. and Zhan, R. B.: Ordovician in the western Yangtze region, South China Palaeoplate: An outline, Palaeoworld, 32, 197–201, https//doi.org/10.1016/j.palwor.2023.03.008, 2023.

Wang, G. X., Cui, Y. N., Liang, Y., Wu, R. C., Wei, X., Gong, F. Y., Huang, B., Luan, X. C., Tang, P., Li, L. X., Zhang, X. L., Zhang, Y. C., Zhang, Z. T., Wang, Q., and Zhan, R. B.: Toward a unified and refined Ordovician stratigraphy for the western Yangtze region, South China, Palaeoworld, 32, 202–218, https//doi.org/10.1016/j.palwor.2022.04.003, 2023.

Wang, X. F.: Ordovician tectonic-paleogeography in South China and chrono-and bio-stratigraphic division and correlation, Earth Sci. Front., 23, 253–267, https://doi.org/10.13745/j.esf.2016.06.018, 2016 (in Chinese with English abstract).

Wang, Z. H. and Wu, R. C.: Ordovician conodont diversification of the Lower Yangteze region, Acta Micropalaeontologica Sinica, 26, 331–350, 2009 (in Chinese).

Wang, Z. H., Bergström, S. M., and Lane, H. R.: Conodont provinces and biostratigraphy in Ordovician of China, Acta Palaeontol. Sin., 1, 133–136, https://doi.org/10.19800/j.cnki.aps.1996.01.002, 1996.

Wang, Z. H., Bergström, S. M., Zhen, Y. Y., Zhang, Y. D., and Wu, R. C.: New conodont data from the Lower Ordovician of Tangshan, Hebei Province, North China, Acta Micropalaeontologica Sinica, 31, 1–14, 2014 (in Chinese with English abstract).

Wang, Z. H., Zhen Y. Y., Zhang, Y. D., and Wu, R. C.: Review of the Ordovician conodont biostratigraphy in the different facies of North China, Journal of Stratigraphy, 40, 1–16, 2016 (in Chinese with English abstract).

Wang, Z. H., Zhen, Y. Y., Bergström, S. M., Wu, R. C., Zhang, Y. D., and Ma, X.: A new conodont biozone classifification of the Ordovician System in South China, Palaeoworld, 28, 173–186, https//doi.org/10.1016/j.palwor.2018.09.002, 2019.

Webers, G. F.: The Middle and Upper Ordovician conodont faunas of Minnesota, Minnesota Geological Survey, 4, 123, 1966.

Wu, R. C. andWang, Z. H.: Lower toMiddle Ordovician conodonts from the Zitai Formation of Shitai, Anhui Province, China, Acta Micropalaeontol. Sin., 25, 364–383, https://doi.org/10.3969/j.issn.1000-0674.2008.04.005, 2008 (in Chinese with English abstract).

Wu, R. C., Zhan, R. B., and Li, G. P.: Conodont diversification in the Zitai Formation (Floian-Dapingian, late early-early mid Ordovician) of Shitai, Anhui Province, East China, Acta Palaeontologica Sinica, 47, 444–453, 2008 (in Chinese with English abstract).

Wu, R. C., Stouge, S., Percival, I. G., and Zhan, R. B.: Early-Middle Ordovician conodont biofacies on the Yangtze Platform margin, South China: Applications to palaeoenvironment and sea-level changes, J. Asian Earth Sci., 96, 194–204, https//-doi.org/10.1016/j.jseaes.2014.09.003, 2014.

Zhan, R. B. and Jin, J. S. (Eds): Ordovician-Silurian (Llandvery) Stratigraphy and Palaeontology of the Upper Yangtze Platform, South China, Science Press, Beijing, China, 25 pp., ISBN 978-7-03-018893-9/Q.1845, 2007.

Zhan, R. B., Ji, J. S., and Liu, J. B.: Investigation on the great Ordovician biodiversification event (GOBE): Review and prospect, Chinese Sci. Bull., 58, 3357–3371, 2013 (in Chinese).

Zhang, Y. B., Zhou, Z. Y., and Zhang, J. M.: Sedimentary differentiation during the latest Early Ordovician-earliest Darriwilian in the Yangtze Block, Journal of Stratigraphy, 26, 302–304, 2002 (in Chinese, with English abstract).

Zhang, Y. D., Zhan, R. B., Zhen, Y. Y., Wang, Z. H., Yuan, W. W., Fang, X., Ma, X., and Zhang, J. P.: Ordovician integrative stratigraphy and timescale of China, Scientia Sinica (Terrae), 49, 66–92, 2019 (in Chinese).

Zhao, Z. X. and Tan, Z. J.: Biostratigraphy of Ordovician in cover area of Tarim Basin, Xinjiang Petroleum Geology, 06, 493–500, 1999 (in Chinese).

Zhen, Y. Y. and Percival, I. G.: Ordovician conodont biogeography-reconsidered, Lethaia, 36, 357–370, https://doi.org/10.1080/00241160310006402, 2003.

Zhen, Y. Y., Percival, I. G., and Liu, J. B.: Early Ordovician Triangulodus (Conodonta) from the Honghuayuan Formation of Guizhou, South China, Alcheringa, 31, 191–212, https//-doi.org/10.1080/03115510608619313, 2006.

Zhen, Y. Y., Percival, I. G., and Webby, B. D.: Discovery of Iapetognathus fauna from far western New South Wales: Towards a more precisely defined Cambrian-Ordovician boundary in Australia, Aust. J. Earth Sci., 64, 487–496, https//-doi.org/10.1080/08120099.2017.1321043, 2017.

Zhu, M. Y., Babcock, L. E., and Peng, S. C.: Advances in Cambrian stratigraphy and paleontology: Integrating correlation techniques, paleobiology, taphonomy and paleoenvironmental reconstruction, Palaeoworld, 15, 217–222, https//-doi.org/10.1016/j.palwor.2006.10.016, 2006.

Zhu, Z. L., Xu, H. K., Chen, X., and Chen, J. Y.: Early Paleozoic strata in Chuxian, Quanjiao, Nanjing and Liuhe areas, Anhui, Series of Nanjing Institute of Geology and Palaeontology, Chinese Academy of Sciences, 7, 135–170, 1984 (in Chinese).